ONCOGENE-EXPRESSING SENESCENT MELANOCYTES UPREGULATE MHC CLASS II, A CANDIDATE MELANOMA SUPPRESSOR FUNCTION

John van Tuyn[a], Farah Jaber-Hijazi[a], Douglas MacKenzie[a], John J. Cole[a], Elizabeth Mann[e], Jeff S. Pawlikowski[b], Taranjit Singh Rai[c], David M. Nelson[a], Tony McBryan[a], Andre Ivanov[d], Karen Blyth[f], Hong Wu[g], Simon Milling[e], Peter D. Adams[a, h]

Affiliations:

A: Institute of Cancer Sciences. University of Glasgow. Garscube Estate. Switchback Road. Glasgow G61 1BD, United Kingdom.

B: Vanderbilt University Medical Center. Nashville, Tennessee, USA.

C: Institute of Biomedical and Environmental Health Research. University of the West of Scotland. Paisley PA1 2BE, United Kingdom.

D: Barts Cancer Institute. Queen Mary, University of London. Charterhouse Square, London EC1M 6BQ, United Kingdom.

E: Institute for Infection, Immunity and Inflammation, University of Glasgow. Glasgow G12 8TA, United Kingdom.

F: Beatson Institute for Cancer Research, Garscube Estate. Switchback Road. Glasgow G61 1BD, United Kingdom.

G: Fox Chase Cancer Center, 333 Cottman Avenue, Philadelphia, PA 19111, USA

H: Sanford Burnham Prebys Medical Discovery Institute, San Diego, CA, USA

Short title: Oncogene-carrying melanocytes activate MHC II

Contact: Peter D. Adams, p.adams@beatson.gla.ac.uk

ABSTRACT

On acquisition of an oncogenic mutation, primary human and mouse cells can enter oncogene-induced senescence (OIS). OIS is characterized by a stable proliferation arrest and secretion of pro-inflammatory cytokines and chemokines, the senescence-associated secretory phenotype (SASP). Proliferation arrest and the SASP collaborate to enact tumor suppression, the former by blocking cell proliferation and the latter by recruiting immune cells to clear damaged cells. However, the interactions of OIS cells with the immune system are still poorly defined. Here we show that engagement of OIS in primary human melanocytes, specifically by melanoma driver mutations *NRASQ61K* and *BRAFV600E*, causes expression of the MHC class II antigen presentation apparatus, via secreted IL1ß signaling and expression of CIITA, a master regulator of MHC class II gene transcription. *In vitro*, OIS melanocytes activate T cell proliferation. *In vivo*, non-proliferating, oncogene-expressing melanocytes localize to skin-draining lymph nodes where they induce T cell proliferation and an antigen presentation gene expression signature. In patients, expression of MHC class II in melanoma is linked to favorable disease outcome. We propose that OIS in melanocytes is accompanied by an antigen presentation phenotype, likely to promote tumor suppression via activation of the adaptive immune system.

Key words: antigen presentation / CIITA / interleukin 1 / melanoma / MHC class II / senescence

INTRODUCTION

Melanoma is a frequently fatal cancer originating from pigment producing melanocytes of the skin (Lo and Fisher, 2014). The most common mutations found in melanoma are those that activate the MAP-kinase signaling pathway, most notably in *BRAF* and *NRAS* (Lo and Fisher, 2014). The same mutations are also commonly found in benign nevi (or moles) (Omholt et al., 2002, Pollock et al., 2003). However, benign nevi only rarely progress to cancer because oncogene-expressing nevus melanocytes are ultimately checked in a proliferation arrested stated, called oncogene-induced senescence (Munoz-Espin and Serrano, 2014). Nevus melanocytes express several molecular markers of senescence, including senescence-associated ß-galactosidase (SA ß-gal) and tumor suppressor p16INK4a (p16) (Gray-Schopfer et al., 2006, Michaloglou et al., 2005, Pawlikowski et al., 2013, Suram et al., 2012). Interestingly, aggregates of apparently non-malignant, non-proliferative, p16-expressing, melanocytic nevus-like cells, in the absence of any concurrent or subsequent melanoma, have also been well documented in the skin draining lymph nodes of humans (Mihic-Probst et al., 2003, Patterson, 2004).

OIS is also characterized by a secretory program, the Senescence Associated Secretory Phenotype (SASP) (Acosta et al., 2008, Krtolica et al., 2001, Kuilman et al., 2008). The SASP has various functions in OIS, including reinforcement and maintenance of proliferation arrest (Acosta et al., 2008, Kuilman et al., 2008), and recruitment of macrophages, neutrophils and NK cells of the innate immune system to clear premalignant oncogene-expressing senescent cells (Xue et al., 2007). NK cells also clear senescent cells in response to other cell and tissue damaging stresses (Krizhanovsky et al., 2008, Soriani et al., 2009). However, clearance of mouse hepatocytes expressing an activated *NrasQ61K* oncogene was also shown to depend on activation of adaptive immunity, specifically on CD4+ T cells (Kang et al., 2011). Typically, CD4+ T cells are activated in the secondary

lymphoid tissues, such as lymph nodes and spleen, by professional antigen presenting cells (APCs), such as dendritic cells (Trombetta and Mellman, 2005). Dendritic cells endocytose and process antigens in peripheral tissues, and then migrate via the lymphatic vessels to the lymph nodes where they activate CD4+ T cells by MHC class II-mediated antigen presentation to naïve T cells.

How senescent cells can activate the adaptive immune systems has been a mystery. Here we show that OIS in melanocytes caused by activation of the RAS/MAP-kinase pathway is accompanied by dramatic upregulation of the MHC class II antigen presentation complex. Furthermore, melanocytes carrying either *BrafV600E* or *NrasQ61K* mutations re-localize specifically to skin-draining lymph nodes in mouse models. We also present functional evidence that in the nodes oncogene-expressing non-proliferating melanocytes enact an antigen presentation function to activate the adaptive immune system.

RESULTS

Melanocytes express MHC class II upon oncogene-induced senescence initiated by melanoma driver mutations.

As we and others previously showed (Michaloglou et al., 2005, Pawlikowski et al., 2013), ectopic expression of BRAFV600E in primary human melanocytes induces OIS. Indicative of senescence, BRAFV600E-expressing melanocytes upregulated SA ß-gal (Figure 1A, 1B), arrested DNA replication as determined by a lack of EdU incorporation (Figure 1B), and showed senescence-associated heterochromatin foci (SAHF) in the nucleus (Figure S1).

We previously investigated the transcriptional changes of melanocytes undergoing OIS by whole genome microarray analysis and RNA-seq analysis (Pawlikowski et al., 2013). Comparing BRAFV600E expressing melanocytes against vector transduced and uninfected melanocytes we observed striking upregulation of MHC class II complex transcripts (Table

S1) (Figure 1C). The cell surface MHC class II complex is a heterodimer of α and ß polypeptides, for example HLA-DRA and HLA-DRB1, respectively. Antigen presentation also depends on expression of chaperones and accessory factors, such as HLA-DM, HLA-D0 and CD74, which facilitate antigen processing, loading and presentation by the MHC class II complex (Trombetta and Mellman, 2005). We observed HLA-DRA and HLA-DRB, amongst the top changes (Table S1). In addition, related HLA-DQA, HLA-DQB, HLA-DPA and HLA-DPB were also upregulated, together with important antigen processing and presentation accessory molecules, such as HLA-DMA, HLA-DMB and invariant chain CD74 (Tables S2 & S3).

Upregulation of the major components of MHC class II mRNAs, HLA-DRA and HLA-DRB, was confirmed by real time-reverse transcription PCR (Figure 1D). Expression of BRAFV600E also enhanced expression of ectopic HLA-DRA and HLA-DRB GFP fusion proteins (Figure 1E). Since this increase is independent of the genes' normal transcription control elements, this also suggests at least some level of post-transcriptional regulation. Expression of endogenous HLA-DR protein in melanocytes upon OIS was demonstrated by Western blot analysis (Figure 1F) and immunofluorescence (Figure 1G, S2). A significant fraction of HLA-DR was localized at the plasma membrane of senescent cells (Figure 1G, S2B), consistent with a role in antigen presentation.

To establish whether BRAFV600E-associated MHC class II expression is cell type restricted, we transduced melanocytes, primary human fibroblasts (IMR90) and primary human epidermal keratinocytes with BRAFV600E or control vector (Figure 2A). In contrast to BRAFV600E transduced melanocytes, neither fibroblasts nor keratinocytes exhibited significant upregulation of MHC class II transcripts levels (Figure 2B). Furthermore, gene expression profiling of fibroblasts transduced with BRAFV600E revealed marked downregulation of proliferation-promoting genes and upregulation of inflammatory/SASP

genes characteristic of senescence (Figure S3), and confirmed no significantly upregulated MHC class II genes (Figure S4). These results together suggest that MHC class II induction is not a common feature of all primary cell types in response to OIS (fibroblasts) and/or oncogene expression (keratinocytes).

In addition to activated oncogenes, other triggers also initiate cell senescence. For example, so-called replicative senescence (RS) which results from excess rounds of cell division (Salama et al., 2014). To test whether MHC class II upregulation is common to different modes of senescence, we investigated RS melanocytes. Melanocytes were serially passaged until they ceased proliferation, and were confirmed to be RS by positive staining for SA ß-gal (Figure 2C, D), and lack of BrdU incorporation (Figure 2D). In contrast to BRAFV600E-mediated OIS, RS did not induce robust upregulation of HLA-DRA or HLA-DRB as detected by qRT-PCR (Figure 2E). Finally, no MHC class II protein could be detected by Western blotting (data not shown). These findings suggest that MHC class II induction is specific to OIS in some cell types, and not RS.

To establish whether MHC class II upregulation in melanocytes is specific to activated BRAFV600E or also triggered by other perturbations of melanoma oncogenic and tumor suppressor pathways, melanocytes were transduced with activated oncogenes, HRASG12V and NRASQ61K, activated MEK1Q56P (Emery et al., 2009) and activated myrAKT, as well as 2 shRNAs to stably knockdown PTEN (Figure 2F). Ectopic expression of each of these oncogenes and knockdown of PTEN resulted in senescence as determined by positive staining for SA ß-gal (Figure 2G left, and Figure S5) and lack of proliferation indicated by the absence of EdU incorporation (Figure 2G right). Expression of NRASQ61K, BRAFV600E and MEK1Q56P resulted in robust upregulation of both HLA-DRA and HLA-DRB, while expression of HRASG12V gave rise to a significantly weaker upregulation of both. In marked contrast, myrAKT expression and PTEN knockdown did not result in

detectable HLA-DR upregulation (Figure 2H). In contrast to results reported here, PTEN knockdown has previously been reported to not cause induction of senescence (Vredeveld et al., 2012). There could be many reasons for this apparent discrepancy – genetic and/or epigenetic differences in the melanocytes, cell culture conditions and others. Regardless, these results suggest that, at least under conditions used here, MHC class II induction is specific to aberrant mitogenic signaling through the RAS/BRAF/ERK pathway, but not the PTEN-AKT signaling pathway.

Since MHC class II induction in BRAFV600E mutant melanocytes occurs concomitantly with induction of senescence, we wished to elucidate whether MHC class II induction is dependent on known effectors of the senescence program. In human cells, an intact p53 or pRB tumor suppressor pathway is necessary for initiation and maintenance of the senescence program (Salama et al., 2014), and abolition of p53/pRB signaling by ectopic expression of SV40 T-antigen disrupts most, if not all, hallmarks of senescence (Shay et al., 1991). To test whether MHC class II induction is abolished by ectopic expression of SV40 T-antigen, we co-expressed BRAFV600E together with SV40 T-antigen (Figure 2I). As expected, T-antigen prevented the growth arrest and SA ß-gal staining associated with senescence in BRAF expressing melanocytes (Figure 2J and S6). Moreover, co-expression of SV40 T-antigen abolished virtually all of the MHC class II induction (Figure 2K). This suggests that MHC class II induction is not only initiated by expression of oncogenic BRAFV600E, but requires at least some elements of the p53 / pRB-dependent senescence effector pathways.

MHC class II upregulation is mediated by an IL1ß-CIITA signaling loop.

Even though expression of SV40 T antigen suppressed induction of HLA-DRA and HLA-DRB (Figure 2I-K), it is well documented that MHC class II expression is typically found in

50-60% of freshly isolated melanoma (Taramelli et al., 1986). We exploited this observation from the melanocytic lineage to gain insight into candidate regulators of MHC class II in primary human melanocytes. We assessed the correlation between mRNA expression of HLA-DRA and HLA-DRB and all other genes in publicly available TCGA skin cutaneous melanoma gene expression datasets (http://cancergenome.nih.gov/). This showed that, across all these datasets, expression of both HLA-DRA and HLA-DRB correlated most strongly with other HLA molecules (e.g. HLA-DQ and HLA-DP), other molecules involved in antigen presentation (e.g. CD74), and CIITA, a transcription factor already known to drive expression of HLA-DRA and HLA-DRB in dendritic cells (Figure 3A, B) (Muhlethaler-Mottet et al., 1997). Conversely, expression of CIITA correlated most strongly with expression of MHC class II antigen presentation molecules (Figure 3A, B). To confirm this correlation, we analyzed RNA-seq data from 7 different melanoma derived cell lines (Pawlikowski et al., 2013) and found that CIITA transcript levels correlated strongly with HLA-DRA and HLA-DRB levels across this panel of melanoma lines (Figure 3C). Moreover, we found that MHC class II induction in melanocytes upon BRAFV600E-mediated OIS is also accompanied by increased CIITA expression (Figure 3D). Like expression of MHC class II, oncogene-induced expression of CIITA was abolished by SV40 T-antigen (Figure 3E). Consistent with upregulation of MHC class II in OIS melanocytes, but not other modes of senescence (Figure 2), we did not observe upregulation of CIITA in OIS fibroblasts (Figure S4). Together, these data from melanoma tumors, cell lines and primary human melanocytes indicate that CIITA is a likely driver of HLA-DRA and HLA-DRB in OIS primary human melanocytes.

In cells known to conditionally express CIITA, expression is frequently induced by extracellular ligands (Trombetta and Mellman, 2005). Significantly, naïve melanocytes exposed to medium from OIS melanocytes upregulated CIITA transcripts (Figure 4A), in conjunction with MHC class II expression (Figure 4A). To identify the extracellular factors

responsible for upregulation of CIITA and MHC class II expression, we probed conditioned medium with an antibody array. Medium from BRAFV600E OIS melanocytes contained increased amounts of inflammatory cytokines compared to conditioned medium from proliferating cells (Figure 4B and Table S4), including interleukin 1B (IL1ß) (in the form of either uncleaved pro-IL1ß or cleaved mature IL1ß), CCL7, CXCL5, CXCL1, VEGF and CCL5. The presence of one or more IL1ß (180 +/- 9 pg/ml, n=4) isoforms in the extracellular medium of OIS melanocytes was confirmed by ELISA (Figure 4C), and robust upregulation of IL1ß mRNA transcripts was detected by qPCR (Figure 4D). When added as recombinant proteins to primary human melanocytes, from a panel of secreted cytokines, only mature IL1ß was able to induce CIITA and MHC class II expression (Figure 4E), but without accompanying activation of senescence, as evidenced by lack of SA ß-gal staining and unimpeded DNA synthesis (Figure 4F). Conversely, partial knockdown of IL1ß using 3 independent shRNAs (Figure 4G) reduced MHC class II induction by BRAFV600E (Figure 4G). Although we have not formally confirmed secretion of cleaved mature IL1ß in this study (rather than uncleaved pro-IL1ß), previous studies have shown that OIS cells do secrete processed mature IL1ß (Acosta et al., 2013), and IL1α and IL1ß are key upstream regulators of the SASP (Acosta et al., 2013, Orjalo et al., 2009). In sum, consistent with these previous studies, our studies indicate a central role for extracellular IL1ß in induction of MHC class II.

We next tested whether IL1ß-mediated upregulation of MHC class II also depends on CIITA. In support of this idea, stimulation of melanocytes with IFNγ, a well-known inducer of CIITA (Trombetta and Mellman, 2005), also upregulated expression of HLA-DRA and HLA-DRB (Figure S7). More pointedly, partial knockdown of CIITA using 2 different shRNAs (Figure 4H) inhibited HLA-DRA and HLA-DRB expression induced by recombinant IL1ß (Figure 4H). Knock down of CIITA with 2 different shRNAs also tended to decrease BRAFV600E-induced expression of HLA-DRA and HLA-DRB, and with the

most effective shRNA, the effect on HLA-DRB expression was significant ($P<0.05$) (Figure 4I). The reduced effectiveness of CIITA knock down in blocking the effects of activated BRAF compared to IL1ß suggests that BRAFV600E can act via additional signaling effectors besides CIITA. Consistent with an IL1ß-CIITA-MHC II pathway, ectopic expression of CIITA was sufficient to induce expression of HLA-DRA and HLA-DRB, but not IL1ß, in melanocytes (Figure 4J). Together, these results indicate that IL1ß-induced expression of CIITA is a major pathway for expression of MHC class II in OIS melanocytes. Interestingly, BRAFV600E-expressing fibroblasts upregulate IL1ß, but neither CIITA nor MHC II (Figure S4). This suggests that functional coupling between IL1ß and CIITA occurs in OIS melanocytes, but not fibroblasts.

Oncogene activation causes localization of melanocytes to lymph nodes and T cell activation.

Previously a mouse model expressing activated NRASQ61K in melanocytes under control of a tyrosinase promoter (*Tyr-NrasQ61K*) was shown to be hyper pigmented due to an excess of melanocytes in the skin, but also to contain melanocytes in the lymph nodes (Ackermann et al., 2005). Extending this observation in these mice, we showed that infiltration of pigmented melanocytes occurs into skin draining (Figure 5A, inguinal and brachial) nodes, but not into non-skin draining nodes (Figure 5A, mesenteric) and spleen (Figure 5A, spleen). While IHC analysis showed melanotic material dispersed throughout the skin draining lymph nodes, particularly in older mice (Figure 5A), immunofluorescence analysis in lymph nodes of albino *Tyr-NrasQ61K* (but not wild type) mice showed cells expressing the melanocyte marker, DCT, and exhibiting dendritic features characteristic of melanocytes predominantly localized adjacent to the subcapsular sinus of the lymph node (Figure 5B and Figure S8A). Therefore, to some extent, the melanotic material in the interior cortex of the node might

reflect residual cell debris, including melanin (oxidized tyrosine polymers), after phagocytic digestion of melanocytes. To eliminate the possibility that localization of melanocytes to lymph nodes is unique to *Tyr-NrasQ61K* mice, we also confirmed in another mouse model of inducible BRAFV600E in melanocytes (*Tyr-Cre-Er : LSL-BrafV600E*) (Mercer et al., 2005) that 4 weeks after oncogene activation, predominantly in the skin of young adult mice (through topical application of tamoxifen), melanocytes also accumulated in skin-draining brachial and inguinal lymph nodes (Figure S8B).

As noted previously (Ackermann et al., 2005), in comparison to wild type mice, the lymph nodes of *Tyr- NrasQ61K* mice were enlarged (Figure 5C and Figure S8C) and their size progressively increased over at least the first several months after birth (Figure 5C). Moreover, the *Tyr-NrasQ61K* mice exhibited more melanocytes in the nodes than the *Tyr-Cre-Er : LSL-BrafV600E* mice (compare Figure 5A and S8B, *NrasQ61K* and *BrafV600E*), paralleling the relative numbers of melanocytes in the skin of each model (Ackermann et al., 2005, Dhomen et al., 2009).

To determine the proliferative status of the melanocytes in the lymph nodes we used 2-color immunofluorescence to stain melanocyte-containing lymph nodes of wild type and *Tyr-NRasQ61K* albino mice for Ki67, a marker of cycling cells, and DCT, a marker of melanocytes. DCT-positive melanocytes in lymph nodes were invariably Ki67-negative, whereas large numbers of surrounding lymphocytes stained positive for Ki67 (Figure 5D). In fact, quantification of the cell fractions from the nodes, showed a massive expansion of non-melanocyte (non-melanin containing) cells (Figure 5E, left) and of CD3+ T cells in particular (Figure 5E, right), suggesting that the melanocytes present in the lymph nodes, directly or indirectly, induce a marked activation and expansion of T cells in these nodes. In sum, the increase in lymph node size appears to result primarily from expansion of T cell populations in melanocyte-containing nodes.

T cell activation and proliferation can be stimulated by MHC class II-mediated antigen presentation (Trombetta and Mellman, 2005). To investigate whether MHC class II-expressing melanocytes acquire the ability to activate T cells, we performed the mixed leukocyte reaction (MLR) in which antigen presenting cells stimulate proliferation of T cells. Indeed, BRAFV600E-expressing OIS melanocytes induced cell division in CSFE labeled CD3+ cells *in vitro*, much more efficiently than control melanocytes (2.3 fold, $p<0.0001$; Figure 5F-G). Although this assay using unpurified T cells does not allow us to attribute T-cell activation to a direct physical interaction between T cells and MHC II on melanocytes, it does show that BRAFV600E mutant melanocytes are more able, either directly by physical interaction or indirectly via other cell types or secreted factors, to stimulate T-cells than are control melanocytes.

To investigate whether melanocyte-containing lymph nodes of *Tyr-NRasQ61K* mice exhibited features of increased antigen presentation, we harvested RNA from lymph nodes and performed RNA-seq. This showed up and down regulation of approximately 577 and 423 genes respectively (Figure S9). Remarkably, the top 5 gene ontologies represented in the upregulated genes of *Tyr-NRasQ61K* nodes reflected increased antigen presentation and associated processes, such as endocytosis and vesicle-mediated transport (Figure 5H,5I). In principle, T cell expansion and antigen presentation in lymph nodes of *Tyr-NrasQ61K* mice could be associated with immune activation or induction of immune tolerance, the latter by activation of Treg cells (Delacher et al., 2014). To distinguish between these possibilities, we stained lymph nodes for expression of FoxP3, a transcription factor expressed by Treg cells (Delacher et al., 2014). This did not reveal an increase in the frequency of Treg cells in lymph nodes from *Tyr-NrasQ61K* mice (Figure 5J). We conclude that oncogene-expressing, non-proliferating primary melanocytes, directly or indirectly, facilitate an antigen presentation function and potential immune activation function in the lymph nodes.

To assess the significance of MHC class II expression in human melanocytic neoplasia, we mined human melanoma TCGA data comparing expression of CIITA, HLA-DRA and HLA-DRB with patient survival. Remarkably, high expression of each of these genes predicted improved patient survival (Figure S10). Moreover, HLA-DRA and HLA-DRB are both components of the recently defined "immune infiltration" gene expression signature that is associated with good prognosis in this disease ((TCGA, 2015), data not shown). Of course, at least part of the CIITA, HLA-DRA and HLA-DRB could be expressed by infiltrating immune cells themselves. However, previous studies have reported expression of HLA-DR on melanoma cells (Barbieri et al., 2011, Colloby et al., 1992, Pollack et al., 1981), and we also confirmed expression of HLA-DRA, HLA-DRB and CIITA in a number of melanoma cell lines (Figure 3C). This underscores the importance of MHC class II expression in melanoma and is consistent with a tumor suppressor role for MHC class II.

DISCUSSION

Here we show that oncogene activation in primary human melanocytes is accompanied by upregulation of MHC class II antigen presentation molecules, and phenotypes and functions suggestive of an antigen presentation role *in vivo*. Upregulation of MHC class II molecules in OIS melanocytes is triggered by SASP factor IL1ß, followed by IL1ß-mediated upregulation of CIITA, a master regulator of MHC class II expression (Trombetta and Mellman, 2005).

Several observations suggest that MHC class II expression in oncogene-expressing melanocytes has a dedicated function. First, melanocytes are restricted to the skin draining nodes, suggesting that they reach the nodes specifically via the lymphatics, the normal route for migration of antigen-presenting dendritic cells, not non-specifically via the blood. Second, these cells do not appear to be malignant, as judged by the absence of proliferation and their routine occurrence in mice lacking any detectable melanoma. Both the *NRas* and *Braf* models

exhibit a long latency in progression to melanoma, of several months to more than a year (Ackermann et al., 2005, Dhomen et al., 2009). In both models, melanocytes were detected in nodes months before any melanoma was detected and is expected (e.g. at 39 days old). As noted previously, aggregates of apparently non-malignant, non-proliferative, p16-expressing, melanocytic nevus-like cells, in the absence of any concurrent or subsequent melanoma, have also been reported in the skin draining lymph nodes of humans (Mihic-Probst et al., 2003, Patterson, 2004) (albeit not as frequently or markedly as observed in the *Tyr-NrasQ61K* mouse model). Third, oncogene-expressing primary melanocytes appear to promote activation of the immune system. Oncogene-expressing senescent melanocytes stimulated T cell proliferation *in vitro* in the MLR assay and localization of melanocytes to the nodes was accompanied by a large increase in node-resident CD3+ T cells. RNA-seq analysis of lymph nodes also revealed gene expression signatures characteristic of increased antigen presentation in the melanocyte-containing lymph nodes of *Tyr-NrasQ61K* mice. The increase in T cells was not accounted for by an overt increase in FoxP3-expressing tolerance-inducing Treg cells. In sum, while we cannot, of course, formally rule out the possibility that the node melanocytes are very early and/or failed micrometastases, the collective data from mice and humans at least suggest the possibility that oncogene-expressing pre-malignant melanocytes might be programmed to activate the adaptive immune system.

Other caveats should also be considered. In general, benign human nevi do not express MHC II, nor are they associated with immune infiltration (Campoli et al., 2012, Lyle et al., 2000). By IHC, we also found that nevi only very rarely (<10%) express detectable MHC II. Conceivably, benign human nevi represent a subset of OIS melanocytes that have been selected for downregulation of MHC II via evasion of MHC II-mediated immune-editing. In apparent contrast to the data presented here, Vemurafenib, a BRAFV600E inhibitor, was previously found to upregulate interferon-mediated MHC II expression in

A375 melanoma cells (Sapkota et al., 2013). A wider comparison of the functional relationship between BRAFV600E and expression of MHC II in transformed melanoma cells, as compared to primary OIS melanocytes primarily studied here, is justified.

Notwithstanding these caveats and the overall complexity of immune responses, comprised of intricate temporally and spatially controlled antagonistic and synergistic interactions between many cell types, these data suggest a model whereby oncogene-expressing primary melanocytes upregulate expression of MHC class II via an IL1ß /CIITA autocrine loop. These melanocytes re-localize to the skin draining lymph nodes where they appear able to directly or indirectly stimulate proliferation of T cells. We propose that the ability of oncogene-expressing primary melanocytes to engage the adaptive immune system may facilitate tumor suppression.

MATERIALS AND METHODS

Details of materials and methods are available in SI Materials and Methods.

Cell culture

Lightly pigmented neonatal human epidermal melanocytes, human neonatal epidermal keratinocytes (both from Invitrogen) IMR90 fibroblasts (ATCC) were cultured according to supplier instructions. Infections with Lentiviral vectors were performed as described (Pawlikowski et al., 2013). In all experiments oncogene and control vector transduced cells were kept in culture under selection for 2 weeks before being assayed for senescence and gene expression. Alternatively melanocytes were cultured in medium supplemented with 10 ng/ml recombinant growth factor listed in Figure 4E (all from Gibco) for 6 days.

Genetically Modified Mouse strains

Mice carrying a tyrosinase promoter driven *NrasQ61K* gene (*Tyr-NrasQ61K*) have been described (Ackermann et al., 2005). Mice conditionally expressing the mutant *BrafV600E* gene under control of tyrosinase driven *CRE-ER* (Delmas et al., 2003) (*Tyr-CRE-ER : LSL-BrafV600E*) have also been described (Dhomen et al., 2009). Albino mice carrying the *Tyr-NrasQ61K* allele were generated by cross-breeding with the albino FVB/NJ (Taketo et al., 1991) strain. Control wild type mice were littermate albino mice lacking the *Tyr-NRasQ61K* transgene. All experiments were carried out in compliance with UK Home Office guidelines at the Beatson Institute for Cancer Research (Home Office PCD 60/2607) under project license 60/4079.

Microarray, RNA-seq and TCGA data

Microarray and RNAseq analysis of melanocytes transduced with BRAF600E expression or control vectors has been described (Pawlikowski et al., 2013), sequences are available from www.ncbi.nlm.nih.gov/geo (accession no. GSE46818).

ACKNOWLEDGEMENTS

We thank Billy Clark for RNA-seq analysis; Colin Nixon for immunohistochemistry; Richard Marais, Catrin Pritchard, Friedrich Beermann, Lynda Chin and Marcus Bosenberg for mouse gene alleles; Daniel Peeper for the BRAFV600E oncogene; the Scottish National Blood Transfusion Service (SNBTS) for excess human donor buffy coats. Work in the lab of PDA was funded by CRUK program C10652/A16566. Thanks to all members of the Adams lab for critical discussions.

CONFLICT OF INTEREST

The authors state no conflict of interest.

FIGURE LEGENDS

Figure 1. Melanocytes express MHC class II upon OIS.

A. Staining for SA ß-gal activity (Blue) on vector or BRAF600E transduced melanocytes. Scale=100 μm. The time span of oncogene activation was kept at 2 weeks for all OIS experiments unless indicated otherwise.

B. Quantification of EdU incorporation and SA ß-gal staining. Graph shows means +/- SD, n=3.

C. Representative RNA-seq track showing HLA-DRA sequence reads for control and BRAFV600E transduced melanocytes. Y axis shows sequence tags per million tags; x axis shows position along the HLA-DRA gene (spanning 5,178 base pair), with boxed exons.

D. Detection of HLA-DRA transcript levels by qRT-PCR analysis.

E. Representative IF image of HLA-DRA-GFP (left three panels) and HLA-DRB-GFP (right three panels) fusion protein transduced melanocytes. GFP staining in green, staining for MHC class II in red and nuclei in blue. Scale bar = 200 μm.

F. Western blot showing BRAF, beta-actin (ATCB) and MHC class II (HLA-DR) expression.

G. Confocal IF image of stained for MHC class II (HLA-DR; red), and nuclei (Blue). Scale bar = 10 μm.

All graphs show means +/- SD, n=4.

Figure 2. Expression of MHC class II is specific to melanocytes and OIS.

A. Western blot of BRAFV600E expression in melanocytes, keratinocytes and fibroblasts transduced with a vector encoding BRAFV600E (B) or control vector (V).

B. HLA-DRA and HLA-DRB transcript levels detected by qRT-PCR analysis, in melanocytes (mel), fibroblasts (fib) or keratinocytes (ker). ND = no signal detected.

C. Staining for SA ß-gal activity in melanocytes in exponential growth phase (PD 26) or at replicative senescence (PD 43). Scale bar = 50 µm.

D. Quantification of SA ß-gal and BrdU positive melanocytes.

E. HLA-DRA and HLA-DRB transcript levels in melanocytes detected by qRT-PCR.

F. Western blots of HRASG12V, NRASQ61K, BRAFV600E, MEKQ56P, myrAKT expression and knockdown of PTEN.

G. Quantification of SA ß-gal staining (left) and EdU incorporation (right) of melanocytes transduced as indicated.

H. HLA-DRA and HLA-DRB transcript levels detected by qRT-PCR of melanocytes transduced as indicated.

I. Western blot showing expression of BRAFV600E and SV40 T-antigen.

J. Quantification of SA ß-gal staining and EdU incorporation of melanocytes transduced with BRAFV600E and SV40 T-antigen.

K. HLA-DRA and HLA-DRB transcripts detected by qRT-PCR.

All graphs show means +/- SD, n=4.

Figure 3. CIITA is a candidate regulator of MHC class II in OIS melanocytes.

A. Whole transcriptome expression correlation network centered on CIITA generated from TCGA melanoma RNA-seq data. Genes are represented as nodes and a Pearson Correlation Coefficient (PCC) between two genes of at least 0.6 as an edge (n=375). CIITA is shaded dark red and HLA genes light red. The boxed highlighted region in left panel is shown in right panel.

B. Scatter plots of TCGA melanoma RNA-seq data comparing the expression of CIITA versus HLA-DRA (left) and CIITA versus HLA-DRB1 (right), in 375 patients.

C. Representative UCSC tracks of library normalized RNA-seq expression at HLA-DRA, HLA-DRB1 and CIITA in 7 melanoma cell lines, melanocytes infected with BRAFV600E and uninfected melanocytes. Y axis shows sequence tags per million tags; x axis shows position along the HLA-DRA gene, with boxed exons.

D. qRT-PCR analysis of CIITA transcript levels detected in melanocytes. Graph depicts means +/- SD, n=4.

E. CIITA transcript levels detected by qRT-PCR. Graph depicts means +/- SD, n=4.

Figure 4. Expression of MHC class II is controlled by an IL1ß-CIITA loop.

A. qRT-PCR analysis of CIITA and HLA-DRA transcripts in melanocytes exposed to conditioned medium for 14 days, from mock, vector and BRAFV600E transduced melanocytes. Graphs depict means +/- SD, n=4.

B. Heatmap of cytokines in conditioned culture medium. See Table S4 for fold change and significance in cytokine levels.

C. Quantification by ELISA of IL1ß in conditioned culture medium. Graph shows mean +/- SD, n=4. (* $p < 0.0001$).

D. qRT-PCR analysis of IL1ß transcripts. Graphs depict means +/- SD, n=4.

E. CIITA, HLA-DRA and HLA-DRB transcripts detected by qRT-PCR of mock or cytokine treated melanocytes. Cells were cultured for 6 days in culture medium supplemented with 10 ng/ml of the indicated cytokine. Graph depicts means +/- SD, n=3.

F. Quantification of EdU incorporation and SA ß-gal staining of melanocytes. Graphs are means +/- SD, n=4.

G. qRT-PCR analysis of IL1ß and HLA-DRA transcripts in melanocytes transduced with vector (V) or BRAFV600E (B) in combination with an shRNA to IL1ß or non-targeting control (NTC). Graphs depict means +/- SD, n=4.

H. qRT-PCR analysis of CIITA, HLA-DRA and HLA-DRB transcripts in melanocytes induced with vehicle or recombinant IL1ß and transduced with shRNAs against CIITA or non-targeting control (NTC).

I. qRT-PCR analysis of CIITA, HLA-DRA and HLA-DRB transcripts in melanocytes transduced with vector or BRAFV600E and an shRNA against CIITA or non-targeting control (NTC). Graphs depict means +/- SD, n=4. * $p<0.05$.

J. qRT-PCR analysis of CIITA, HLA-DRA, HLA-DRB and IL1ß transcript levels in melanocytes transduced with control vector (V), BRAFV600E (B) or CIITA (C) over expression vectors. Graphs depict means +/- SD, n=4.

Figure 5. Oncogene expressing melanocytes localize to skin draining lymph nodes.

A. H+E stained sections of lymph nodes and spleen of WT and *Tyr-NrasQ61K* mice. Scale bar = 100 μm.

B. DCT (green)-expressing cells in lymph node. DAPI, blue. Sub S, subcapsular sinus. C, cortex. Scale bar = 100 μm.

C. Inguinal lymph node size plotted against age of mouse. Each point is a single node (2 nodes per mouse).

D. Melanocytes detected by DCT (green) in lymph nodes of albino *Tyr-NrasQ61K* transgenic mice and cycling cells detected by Ki67 (red). Scale bar = 100 μm.

E. Quantification of total non-melanocyte (non-pigmented, left) and CD3+ fraction (right) from pooled inguinal, brachial and axillary lymph nodes per mouse. Graph plots means +/- SD (n=3 per group). * 7.2 fold difference (p=0.0049). # 5.3 fold difference (p=0.0007).

F. FACS analysis of CSFE levels in CD3+ cells after co-culture with WBCs (neg, solid line), WBCs incubated with LPS (LPS), and melanocytes transduced with vector or BRAFV600E. The plot with the neg. sample also shows unstained WBCs (neg, dotted line).

G. Percentage of replicating CD3+ cells after induction with WBCs (neg), WBCs incubated with LPS (LPS), and vector or BRAFV600E transduced melanocytes. Bars represent means +/- SD, n=4.

H. Table of the 5 most enriched gene ontologies (FDR <=5%) for genes that are upregulated by RNA-seq (FDR <= 5%) in *Tyr-NrasQ61K* over WT lymph nodes.

I. Column clustered heatmap of all genes in the ontologies given in H) for WT and *Tyr-NrasQ61K* lymph nodes. Genes are given by column and samples by row. The color intensity represents column Z-Score, where red indicates more highly expressed, and blue more lowly expressed genes.

J. Representative Foxp3 staining (brown) of albino WT and *Tyr-NrasQ61K* mice. Nuclei are counterstained with hematoxylin (blue). Scale bar represents 50 μm. Quantification of the number of positive cells in 2 NRAS61K mice and 2 WT littermates, by calculating the average number positive cells from 2 slides per lymph node and counting 3 lymph nodes (2 Inguinal, 1 brachial) per mouse, showed no significant difference between the nodes (160.8 +/- 21.1 vs. 174.3 +/- 27.6, n=2, p=0.83).

REFERENCES

Ackermann J, Frutschi M, Kaloulis K, McKee T, Trumpp A, Beermann F. Metastasizing melanoma formation caused by expression of activated N-RasQ61K on an INK4a-deficient background. Cancer Res 2005;65(10):4005-11.

Acosta JC, Banito A, Wuestefeld T, Georgilis A, Janich P, Morton JP, et al. A complex secretory program orchestrated by the inflammasome controls paracrine senescence. Nat Cell Biol 2013;15(8):978-90.

Acosta JC, O'Loghlen A, Banito A, Guijarro MV, Augert A, Raguz S, et al. Chemokine signaling via the CXCR2 receptor reinforces senescence. Cell 2008;133(6):1006-18.

Barbieri G, Rimini E, Costa MA. Effects of human leukocyte antigen (HLA)-DR engagement on melanoma cells. Int J Oncol 2011;38(6):1589-95.

Campoli M, Fitzpatrick JE, High W, Ferrone S. HLA antigen expression in melanocytic lesions: Is acquisition of HLA antigen expression a biomarker of atypical (dysplastic) melanocytes? Journal of the American Academy of Dermatology 2012;66(6):911-6.e8.

Colloby PS, West KP, Fletcher A. Is poor prognosis really related to HLA-DR expression by malignant melanoma cells? Histopathology 1992;20(5):411-6.

Delacher M, Schreiber L, Richards DM, Farah C, Feuerer M, Huehn J. Transcriptional control of regulatory T cells. Curr Top Microbiol Immunol 2014;381:83-124.

Delmas V, Martinozzi S, Bourgeois Y, Holzenberger M, Larue L. Cre-mediated recombination in the skin melanocyte lineage. genesis 2003;36(2):73-80.

Dhomen N, Reis-Filho JS, da Rocha Dias S, Hayward R, Savage K, Delmas V, et al. Oncogenic Braf induces melanocyte senescence and melanoma in mice. Cancer Cell 2009;15(4):294-303.

Emery CM, Vijayendran KG, Zipser MC, Sawyer AM, Niu L, Kim JJ, et al. MEK1 mutations confer resistance to MEK and B-RAF inhibition. Proceedings of the National Academy of Sciences of the United States of America 2009;106(48):20411-6.

Gray-Schopfer VC, Cheong SC, Chong H, Chow J, Moss T, Abdel-Malek ZA, et al. Cellular senescence in naevi and immortalisation in melanoma: a role for p16? Br J Cancer 2006;95(4):496-505.

Kang TW, Yevsa T, Woller N, Hoenicke L, Wuestefeld T, Dauch D, et al. Senescence surveillance of pre-malignant hepatocytes limits liver cancer development. Nature 2011;479(7374):547-51.

Krizhanovsky V, Yon M, Dickins RA, Hearn S, Simon J, Miething C, et al. Senescence of Activated Stellate Cells Limits Liver Fibrosis. Cell 2008;134(4):657-67.

Krtolica A, Parrinello S, Lockett S, Desprez P-Y, Campisi J. Senescent fibroblasts promote epithelial cell growth and tumorigenesis: A link between cancer and aging. Proceedings of the National Academy of Sciences 2001;98(21):12072-7.

Kuilman T, Michaloglou C, Vredeveld LCW, Douma S, van Doorn R, Desmet CJ, et al. Oncogene-Induced Senescence Relayed by an Interleukin-Dependent Inflammatory Network. Cell 2008;133(6):1019-31.

Lo JA, Fisher DE. The melanoma revolution: from UV carcinogenesis to a new era in therapeutics. Science 2014;346(6212):945-9.

Lyle S, Salhany KE, Elder DE. TIA-1 Positive Tumor-Infiltrating Lymphocytes in Nevi and Melanomas. Mod Pathol 2000;13(1):52-5.

Mercer K, Giblett S, Green S, Lloyd D, DaRocha Dias S, Plumb M, et al. Expression of endogenous oncogenic V600EB-raf induces proliferation and developmental defects in mice and transformation of primary fibroblasts. Cancer Res 2005;65(24):11493-500.

Michaloglou C, Vredeveld LC, Soengas MS, Denoyelle C, Kuilman T, van der Horst CM, et al. BRAFE600-associated senescence-like cell cycle arrest of human naevi. Nature 2005;436(7051):720-4.

Mihic-Probst D, Saremaslani P, Komminoth P, Heitz PU. Immunostaining for the tumour suppressor gene p16 product is a useful marker to differentiate melanoma metastasis from lymph-node nevus. Virchows Archiv : an international journal of pathology 2003;443(6):745-51.

Muhlethaler-Mottet A, Otten LA, Steimle V, Mach B. Expression of MHC class II molecules in different cellular and functional compartments is controlled by differential usage of multiple promoters of the transactivator CIITA. EMBO J 1997;16(10):2851-60.

Munoz-Espin D, Serrano M. Cellular senescence: from physiology to pathology. Nat Rev Mol Cell Biol 2014;15(7):482-96.

Omholt K, Karsberg S, Platz A, Kanter L, Ringborg U, Hansson J. Screening of N-ras codon 61 mutations in paired primary and metastatic cutaneous melanomas: mutations occur early and persist throughout tumor progression. Clin Cancer Res 2002;8(11):3468-74.

Orjalo AV, Bhaumik D, Gengler BK, Scott GK, Campisi J. Cell surface-bound IL-1α is an upstream regulator of the senescence-associated IL-6/IL-8 cytokine network. Proceedings of the National Academy of Sciences of the United States of America 2009;106(40):17031-6.

Patterson JW. Nevus cell aggregates in lymph nodes. Am J Clin Pathol 2004;121(1):13-5.

Pawlikowski JS, McBryan T, van Tuyn J, Drotar ME, Hewitt RN, Maier AB, et al. Wnt signaling potentiates nevogenesis. Proc Natl Acad Sci U S A 2013;110(40):16009-14.

Pollack MS, Heagney SD, Livingston PO, Fogh J. HLA-A, B, C and DR alloantigen expression on forty-six cultured human tumor cell lines. J Natl Cancer Inst 1981;66(6):1003-12.

Pollock PM, Harper UL, Hansen KS, Yudt LM, Stark M, Robbins CM, et al. High frequency of BRAF mutations in nevi. Nat Genet 2003;33(1):19-20.

Salama R, Sadaie M, Hoare M, Narita M. Cellular senescence and its effector programs. Genes Dev 2014;28(2):99-114.

Sapkota B, Hill CE, Pollack BP. Vemurafenib enhances MHC induction in BRAF homozygous melanoma cells. Oncoimmunology 2013;2(1):e22890.

Shay JW, Wright WE, Werbin H. Defining the molecular mechanisms of human cell immortalization. Biochim Biophys Acta 1991;1072(1):1-7.

Soriani A, Zingoni A, Cerboni C, Iannitto ML, Ricciardi MR, Di Gialleonardo V, et al. ATM-ATR–dependent up-regulation of DNAM-1 and NKG2D ligands on multiple myeloma cells by therapeutic agents results in enhanced NK-cell susceptibility and is associated with a senescent phenotype. Blood 2009;113(15):3503-11.

Suram A, Kaplunov J, Patel PL, Ruan H, Cerutti A, Boccardi V, et al. Oncogene-induced telomere dysfunction enforces cellular senescence in human cancer precursor lesions. The EMBO Journal 2012;31(13):2839-51.

Taketo M, Schroeder AC, Mobraaten LE, Gunning KB, Hanten G, Fox RR, et al. FVB/N: an inbred mouse strain preferable for transgenic analyses. Proc Natl Acad Sci U S A 1991;88(6):2065-9.

Taramelli D, Fossati G, Mazzocchi A, Delia D, Ferrone S, Parmiani G. Classes I and II HLA and Melanoma-associated Antigen Expression and Modulation on Melanoma Cells Isolated from Primary and Metastatic Lesions. Cancer Research 1986;46(1):433-9.

TCGA. Genomic Classification of Cutaneous Melanoma. Cell 2015;161(7):1681-96.

Trombetta ES, Mellman I. Cell biology of antigen processing in vitro and in vivo. Annual Review of Immunology 2005;23(1):975-1028.

Vredeveld LC, Possik PA, Smit MA, Meissl K, Michaloglou C, Horlings HM, et al. Abrogation of BRAFV600E-induced senescence by PI3K pathway activation contributes to melanomagenesis. Genes Dev 2012;26(10):1055-69.

Xue W, Zender L, Miething C, Dickins RA, Hernando E, Krizhanovsky V, et al. Senescence and tumour clearance is triggered by p53 restoration in murine liver carcinomas. Nature 2007;445(7128):656-60.

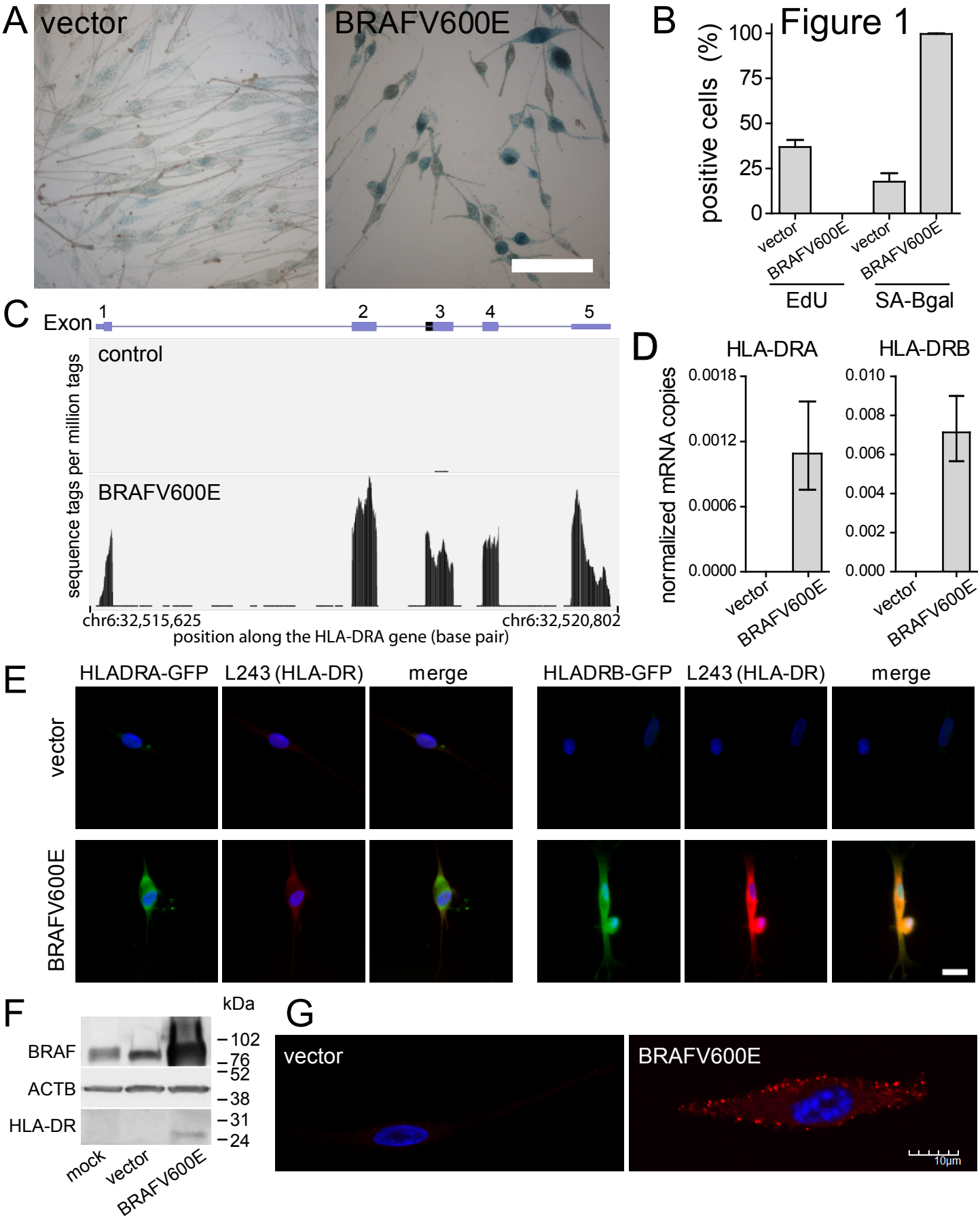
A
vector
BRAFV600E
B
Figure 1
positive cells (%)
100
75
50
25
0
vector
BRAFV600E
vector
BRAFV600E
EdU
SA-Bgal
C
Exon
1
2
3
4
5
control
BRAFV600E
sequence tags per million tags
chr6:32,515,625
chr6:32,520,802
position along the HLA-DRA gene (base pair)
D
HLA-DRA
HLA-DRB
normalized mRNA copies
0.0018
0.0012
0.0006
0.0000
0.010
0.008
0.006
0.004
0.002
0.000
vector
BRAFV600E
vector
BRAFV600E
E
HLADRA-GFP
L243 (HLA-DR)
merge
HLADRB-GFP
L243 (HLA-DR)
merge
vector
BRAFV600E
F
kDa
BRAF
ACTB
HLA-DR
102
76
52
38
31
24
mock
vector
BRAFV600E
G
vector
BRAFV600E
10μm

Figure 2

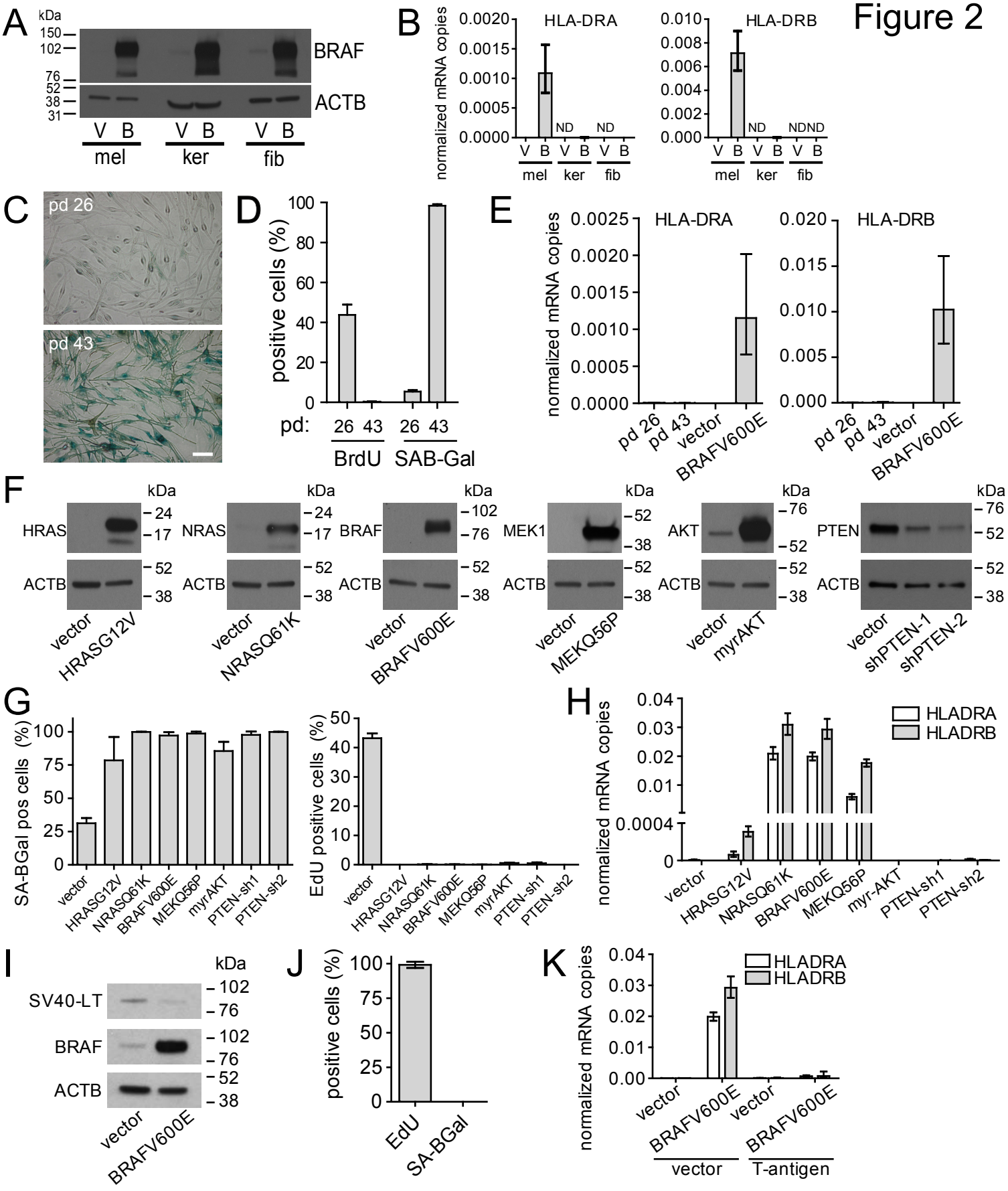
A
kDa
150
102
76
52
38
31
BRAF
ACTB
V B V B V B
mel ker fib
B
normalized mRNA copies
HLA-DRA
HLA-DRB
ND
C
pd 26
pd 43
D
positive cells (%)
pd: 26 43 26 43
BrdU SAB-Gal
E
normalized mRNA copies
HLA-DRA
HLA-DRB
pd 26
pd 43
vector
BRAFV600E
F
HRAS
NRAS
BRAF
MEK1
AKT
PTEN
ACTB
vector
HRASG12V
NRASQ61K
BRAFV600E
MEKQ56P
myrAKT
shPTEN-1
shPTEN-2
G
SA-BGal pos cells (%)
EdU positive cells (%)
vector
HRASG12V
NRASQ61K
BRAFV600E
MEKQ56P
myrAKT
PTEN-sh1
PTEN-sh2
H
normalized mRNA copies
HLADRA
HLADRB
myr-AKT
I
SV40-LT
BRAF
ACTB
vector
BRAFV600E
J
positive cells (%)
EdU
SA-BGal
K
normalized mRNA copies
HLADRA
HLADRB
vector
BRAFV600E
T-antigen

Figure 3

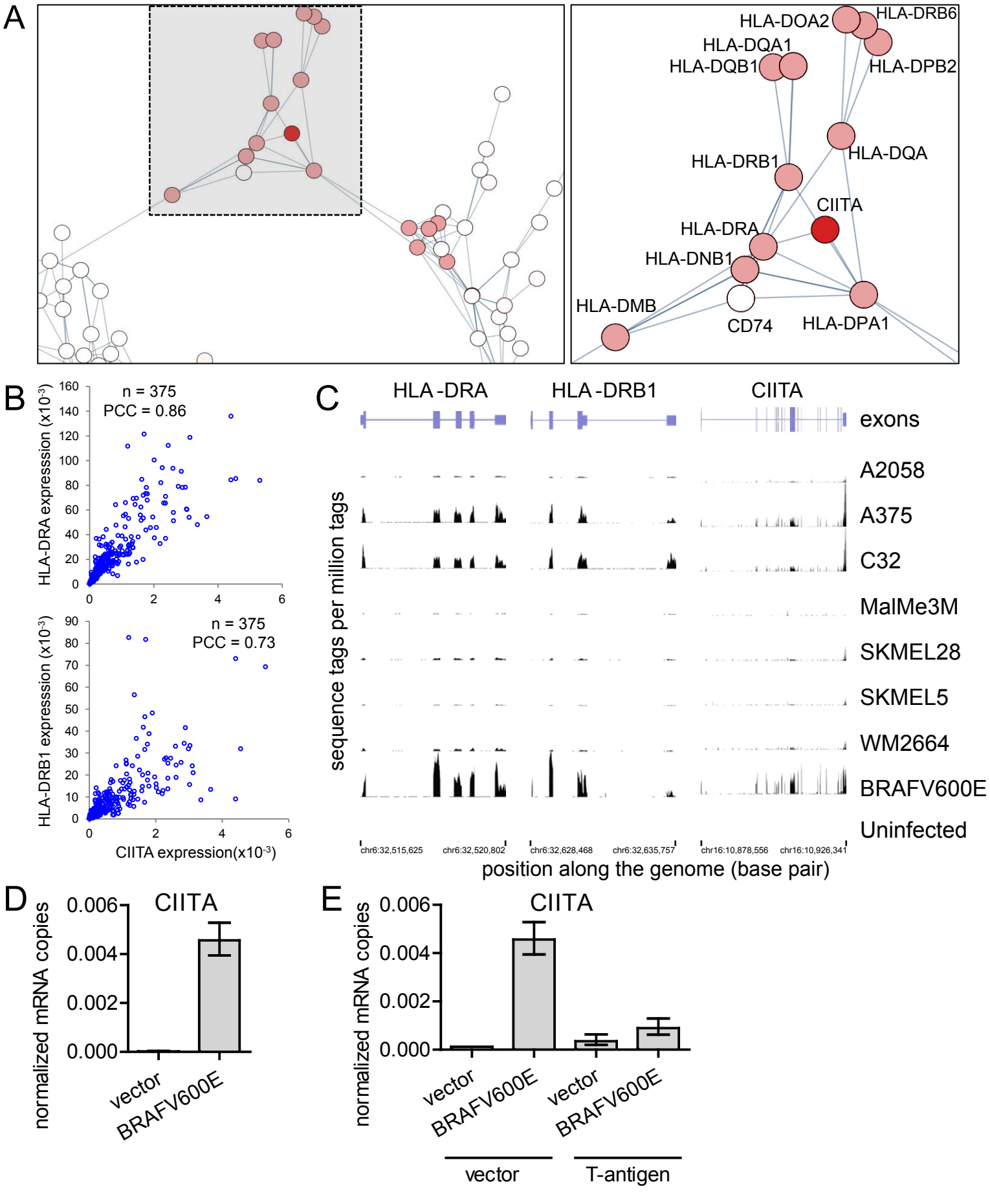
A
HLA-DOA2
HLA-DRB6
HLA-DQA1
HLA-DQB1
HLA-DPB2
HLA-DRB1
HLA-DQA
CIITA
HLA-DRA
HLA-DNB1
HLA-DMB
CD74
HLA-DPA1
B
n = 375
PCC = 0.86
HLA-DRA expresssion (x10-3)
n = 375
PCC = 0.73
HLA-DRB1 expresssion (x10-3)
CIITA expression(x10-3)
C
HLA-DRA
HLA-DRB1
CIITA
exons
A2058
A375
C32
MalMe3M
SKMEL28
SKMEL5
WM2664
BRAFV600E
Uninfected
sequence tags per million tags
chr6:32,515,625
chr6:32,520,802
chr6:32,628,468
chr6:32,635,757
chr16:10,878,556
chr16:10,926,341
position along the genome (base pair)
D
CIITA
normalized mRNA copies
vector
BRAFV600E
E
CIITA
normalized mRNA copies
vector
BRAFV600E
vector
BRAFV600E
vector
T-antigen

Figure 4

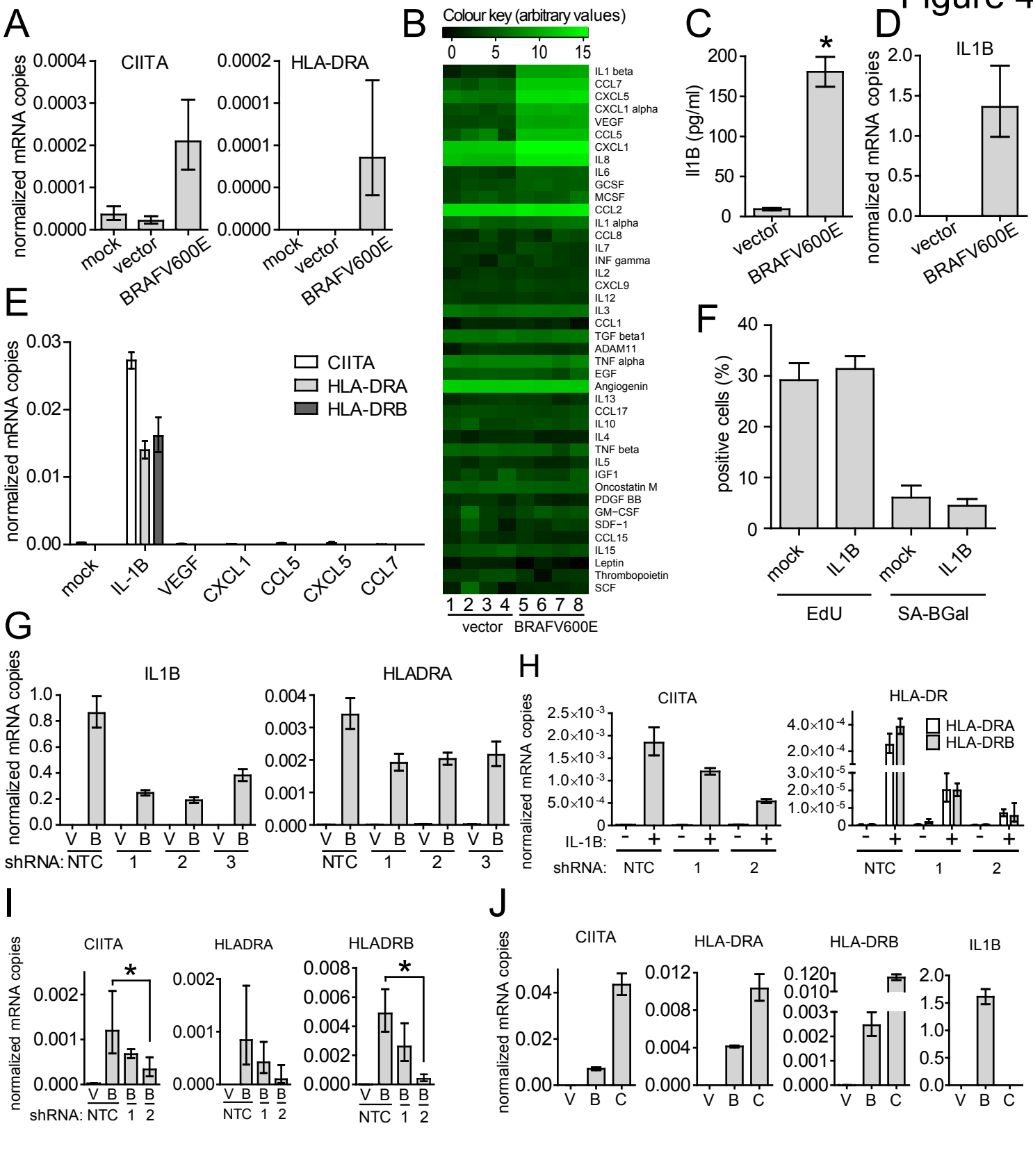
A
CIITA
HLA-DRA
normalized mRNA copies
mock
vector
BRAFV600E
B
Colour key (arbitrary values)
IL1 beta
CCL7
CXCL5
CXCL1 alpha
VEGF
CCL5
CXCL1
IL8
IL6
GCSF
MCSF
CCL2
IL1 alpha
CCL8
IL7
INF gamma
IL2
CXCL9
IL12
IL3
CCL1
TGF beta1
ADAM11
TNF alpha
EGF
Angiogenin
IL13
CCL17
IL10
IL4
TNF beta
IL5
IGF1
Oncostatin M
PDGF BB
GM−CSF
SDF−1
CCL15
IL15
Leptin
Thrombopoietin
SCF
vector
BRAFV600E
C
Il1B (pg/ml)
D
IL1B
E
CIITA
HLA-DRA
HLA-DRB
IL-1B
VEGF
CXCL1
CCL5
CXCL5
CCL7
F
positive cells (%)
EdU
SA-BGal
G
IL1B
HLADRA
shRNA: NTC 1 2 3
H
CIITA
HLA-DR
IL-1B:
shRNA: NTC 1 2
I
CIITA
HLADRA
HLADRB
shRNA: NTC 1 2
J
CIITA
HLA-DRA
HLA-DRB
IL1B

Figure 5

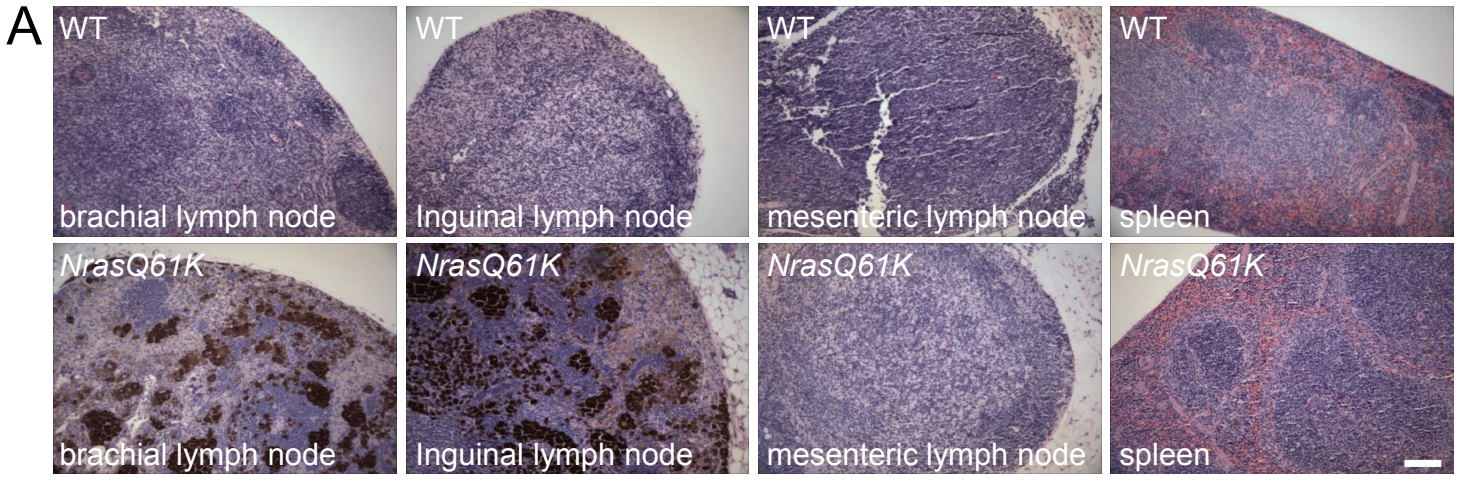

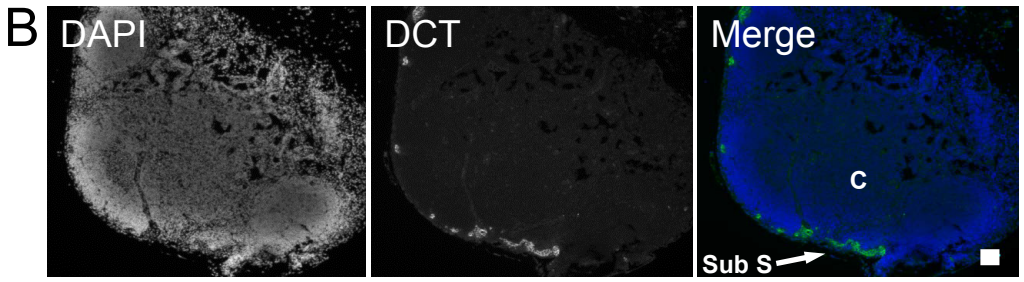

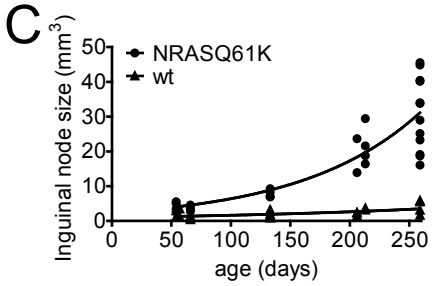

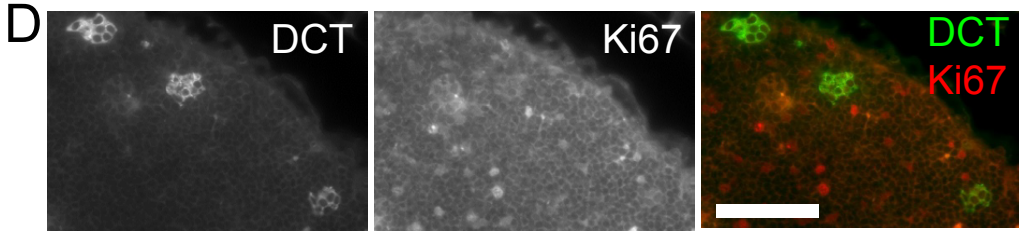

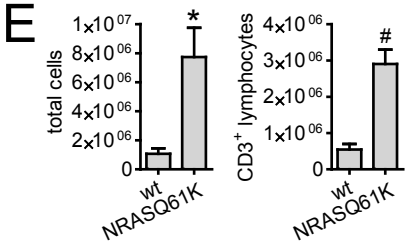

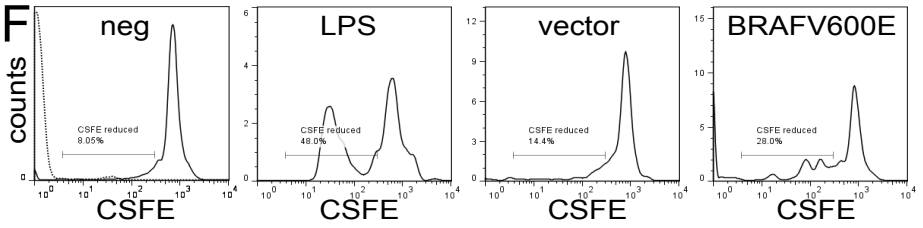

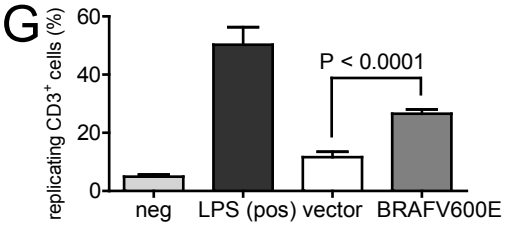

H

Term ID	Term Name	Count	Fold Enrichment	FDR
GO:0050764	regulation of phagocytosis	6	10.49	**0.37%**
GO:0045807	positive regulation of endocytosis	6	7.71	**1.62%**
GO:0048002	antigen processing and presentation of peptide antigen	6	7.49	**1.85%**
GO:0030100	regulation of endocytosis	8	6.72	**0.28%**
GO:0060627	regulation of vesicle-mediated transport	9	4.74	**1.00%**

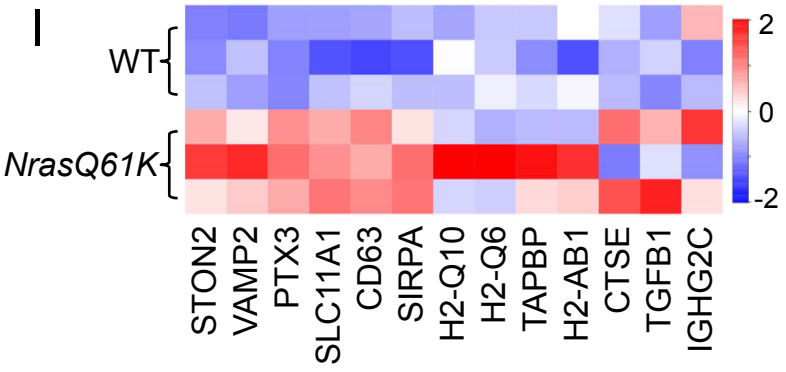

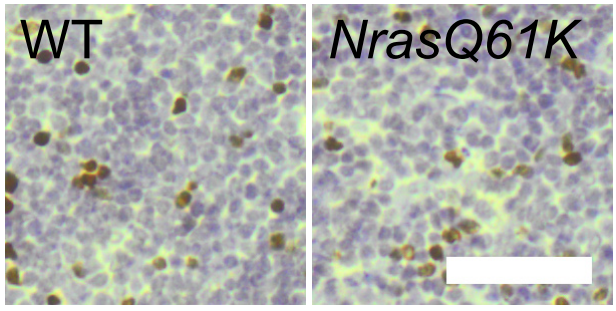

SUPPLEMENTAL DATA

Table S1. Top 20 changes between BRAFV600E and control melanocytes, determined by Affymetrix array and RNAseq.

Affimetrix array[1]				RNAseq[2]		
Gene Symbol	UniGene ID	fold change	p (Holm)	Gene Symbol	locus	fold change
IL1B	Hs.126256	1798	5.80E-04	IL1B	chr2:113303654-113310988	28701
AREG	Hs.270833	1603	7.04E-03	C3	chr19:6628590-6671684	13965
HLA-DRA	Hs.520048	1384	6.57E-04	HLA-DRB1/5	chr6:32549180-32742436	6786
INHBA	Hs.583348	1289	5.58E-03	SERPINB2	chr18:59705918-59722158	6552
NPTX2	Hs.3281	1094	2.69E-03	AL121995.1/3	chr1:119778820-119903801	5922
TFPI2	Hs.438231	1087	9.02E-05	NPTX2	chr7:98099076-98099888	5333
TGFBI	Hs.369397	981	2.20E-04	HLA-DRA	chr6:32515610-32520802	5200
EREG	Hs.115263	886	3.95E-02	TNC	chr9:116821716-116920290	2761
HLA-DRB1/4	Hs.696211	883	1.21E-03	SAA1	chr11:18244360-18248092	2682
INHBA	Hs.583348	843	1.78E-03	TAGLN3	chr3:113200936-113215425	2289
C3	Hs.529053	772	2.95E-03	INHBA	chr7:41691160-41709216	1911
SERPINB2	Hs.594481	719	1.86E-02	TAC1	chr7:97199176-97207721	1885
TFPI2	Hs.438231	654	1.25E-02	HLA-DQB1	chr6:32549180-32742436	1762
COL22A1	Hs.117169	627	1.84E-03	MMP10	chr11:102146454-102156555	1690
CXCR4	Hs.593413	620	1.02E-01	TFPI2	chr7:93349289-93358297	1571
STC1	Hs.25590	613	9.92E-03	LCE1F	chr1:151017002-151017127	1560
ANGPTL4	Hs.9613	571	8.94E-02	MYH15	chr3:109646173-109646434	1402
RTN1	Hs.368626	568	8.39E-03	COL22A1	chr8:139707615-139995421	1327
STC1	Hs.25590	553	3.47E-04	EREG	chr4:75449369-75473334	1263
ANGPTL4	Hs.9613	571	8.94E-02	PRSS3	chr9:33740483-33789331	1244

BRAFV600E and control melanocytes were kept in culture under selection for 1 week before being assayed for senescence and gene expression as described (Pawlikowski et al., 2013), using either Affymetrix array (n=3) or RNA-seq (n=1). The full dataset can be obtained from www.ncbi.nlm.nih.gov/geo (accession no. GSE46818). See also Table S2 and S3 for Antigen presentation related transcript changes, detected by Affymetrix array and RNA-seq respectively.

[1]N=3 replicates. [2]N=1 replicate.

Table S2 . Antigen presentation related transcript changes between BRAFV600E and control melanocytes, determined by Affymetrix array.

Gene symbol	fold change[1,2]	p (Holm)
IL1ß	1797.5	0.001
HLA-DRA	1384.4	0.001
HLA-DRB1/4	883.2	0.001
CD74	250.8	0.016
HLA-DQB1	240.1	0.104
IL1A	237.8	0.002
BRAF	191.9	0.004
HLA-DRB1/3/4	182.9	0.018
IL8	158.0	0.134
IL11	130.7	0.016
HLA-DQA1	95.6	0.014
HLA-DMB	77.5	0.193
HLA-DRB4	46.2	0.256
IL33	32.2	1.000
HLA-DRB6	29.9	1.000
CTLA4	24.4	0.053
CIITA	22.6	0.111
HLA-DOA	15.8	0.107
HLA-DPA1	14.4	0.387
HLA-DMA	8.8	1.000
ICAM1	6.6	1.000
HLA-B	3.0	1.000
HLA-DPB1	3.0	1.000
HLA-DOB	1.8	1.000
CD28	1.8	1.000
HLA-F	1.4	1.000
HLA-C	1.4	0.302
HLA-E	1.3	1.000
HLA-DQB2	1.2	1.000
HLA-A	1.2	1.000
HLA-G	1.1	1.000
CD80	1.1	1.000
ICAM5	1.1	1.000
CD40	-1.1	1.000

[1]N=3. [2]Also see Table S3 for antigen presentation transcript changes detected by RNAseq. See Table S1 for additional information on the dataset.

Table S3. Antigen presentation related transcript changes between BRAFV600E infected and control melanocytes, determined by RNAseq.

Gene Symbol	Fold change[1,2]
IL1ß	28700.6
HLA-DRB1/5	6786.1
HLA-DRA	5199.7
HLA-DQB1	1762.4
HLA-DQA1	1013.4
HLA-DRB5	777.2
IL1A	771.9
HLA-DQA2	391.7
IL8	226.4
CD74	107.6
HLA-DMB	51.0
ICAM5	48.4
HLA-DOA	44.4
HLA-DOB	42.7
CD28	41.5
CIITA	31.7
CTLA4	21.3
HLA-DPA1	16.7
IL33	13.7
HLA-DMA	6.1
ICAM1	6.1
HLA-C	4.3
HLA-DPB1	3.2
HCG4P5,HLA-A	3.0
HLA-A/F	1.6
HLA-E	1.3
CD40	0.7
HHLA3	0.6
HLA-Z	0.5

[1]N=1. [2]Also see Table S2 for antigen presentation transcript changes detected by Affymetrix array. See Table S1 for additional information on the dataset.

Table S4. Mean fold change of cytokine quantities between the conditioned culture medium of BRAFV600E and vector transduced melanocytes.

Name	Fold change	P (Bh-fdr)[1]
IL1 beta	179.6	0.001
CCL7	131.8	0.001
CXCL5	100.1	0.000
CXCL1 alpha	64.0	0.000
VEGF	56.7	0.000
CCL5	33.0	0.035
CXCL1	10.8	0.000
IL8	8.3	0.000
IL6	4.2	0.008
GCSF	2.8	0.004
MCSF	1.9	0.490
CCL2	1.8	0.004
IL1 alpha	1.8	0.164
CCL8	1.6	0.617
IL7	1.6	0.459
INF gamma	1.3	0.620
IL2	1.3	0.557
CXCL9	1.2	0.396
IL12	1.1	0.593
IL3	1.1	0.798
CCL1	1.0	0.955
TGF beta1	1.0	0.955
ADAM11	1.0	0.836
TNF alpha	1.0	0.955
EGF	0.9	0.773
Angiogenin	0.9	0.121
IL13	0.9	0.891
CCL17	0.9	0.620
IL10	0.9	0.955
IL4	0.8	0.620
TNF beta	0.8	0.620
IL5	0.8	0.620
IGF1	0.8	0.955
Oncostatin M	0.8	0.463
PDGF BB	0.8	0.620
GM-CSF	0.8	0.754
SDF-1	0.7	0.955
CCL15	0.7	0.593
IL15	0.7	0.557
Leptin	0.5	0.251
Thrombopoietin	0.4	0.251
SCF	0.2	0.827

[1]Significance was calculated by students t-test with BH-fdr correction (n=4). Cytokine quantities in filtered culture supernatant from BRAFV600E and vector transduced melanocytes were determined using the human cytokine array G series 3 (Raybio). Culture supernatant was collected 2 weeks post transduction, and 2 days since the medium was last replaced.

Table S5. Quality control data of the RNA-seq of mouse WT and NrasQ61K lymph nodes.

Replicate ID	Sample	Raw Sequence reads	Read Length	Aligned Reads (% of Raw Sequence reads)	Non-Duplicate Reads (% of Aligned Reads)
46419	wt	10,004,588	72PE	9,480,699 (94.76%)	8,186,445 (86.35%)
71309	wt	15,607,227	72PE	14,883,831 (95.36%)	13,392,117 (89.98%)
71310	wt	15,929,113	72PE	15,230,797 (95.62%)	12,793,310 (84.00%)
61600	*NrasQ61K*	13,785,721	72PE	12,808,334 (92.91%)	11,633,500 (90.83%)
68718	*NrasQ61K*	10,221,677	72PE	6,967,111 (68.16%)	5,621,199 (80.68%)
68722	*NrasA61K*	13,393,846	72PE	12,646,809 (94.42%)	10,159,113 (80.33%)

Table S6. Primer sequences used for reverse transcription-real time PCR analysis.

Target	Forward primer[1]	Reverse primer[1]	probe[1]
hGAPDH	ACACCCACTCCTCCACCTTT	ATGAGGTCCACCACCCTGT	ATTGCCCTCAACGACCACTTTGTC
hACTB	AGAAGGATTCCTATGTGGGCG	CATGTCGTCCCAGTTGGTGAC	CTCACCCTGAAGTACCCCATCGAG
hCIITA	CACTAACCACGCTGGACCTT	GCAGAGCAAGATGTGGTTCA	CTTCTCCAGGCTGTATCCCATGAGC
hHLA-DRA	CCCAACGTCCTCATCTGTTT	AGCATCAAACTCCCAGTGCT	AAGTTCACCCCACCAGTGGTCAAT
hHLA-DRB	GCACAGAGCAAGATGCTGAG	GCAACCAGGTCCTGAGAAAG	TCCTGAGCTGAAATGCAGATGACC
hIL-1B	GCTGAGGAAGATGCTGGTTC	TCGTTATCCCATGTGTCGAA	TCCAGGAGAATGACCTGAGCACCTTC
mACTB	AGCCATGTACGTAGCCATCC	GCTGTGGTGGTGAAGCTGTA	CATCTACGAGGGCTATGCTCTCCCT
mH2-Ab1	CCTGGTGACTGCCATTACCT	ACGTACTCCTCCCGGTTGTA	TCGTGTACCAGTTCATGGGCGA

[1]All sequences are given 5' to 3'.

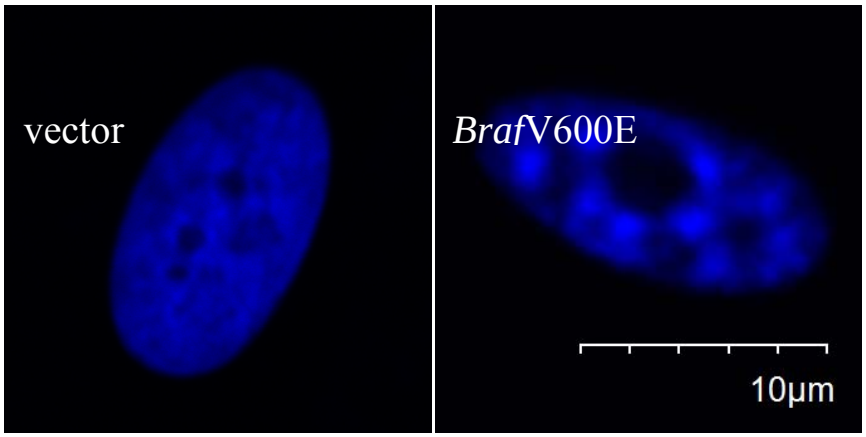

Figure S1. Nuclei of senescent melanocytes display senescence-associated heterochromatin foci (SAHF).

Confocal image of DAPI stained nuclei of vector control and *BRAF*V600E expressing melanocytes.

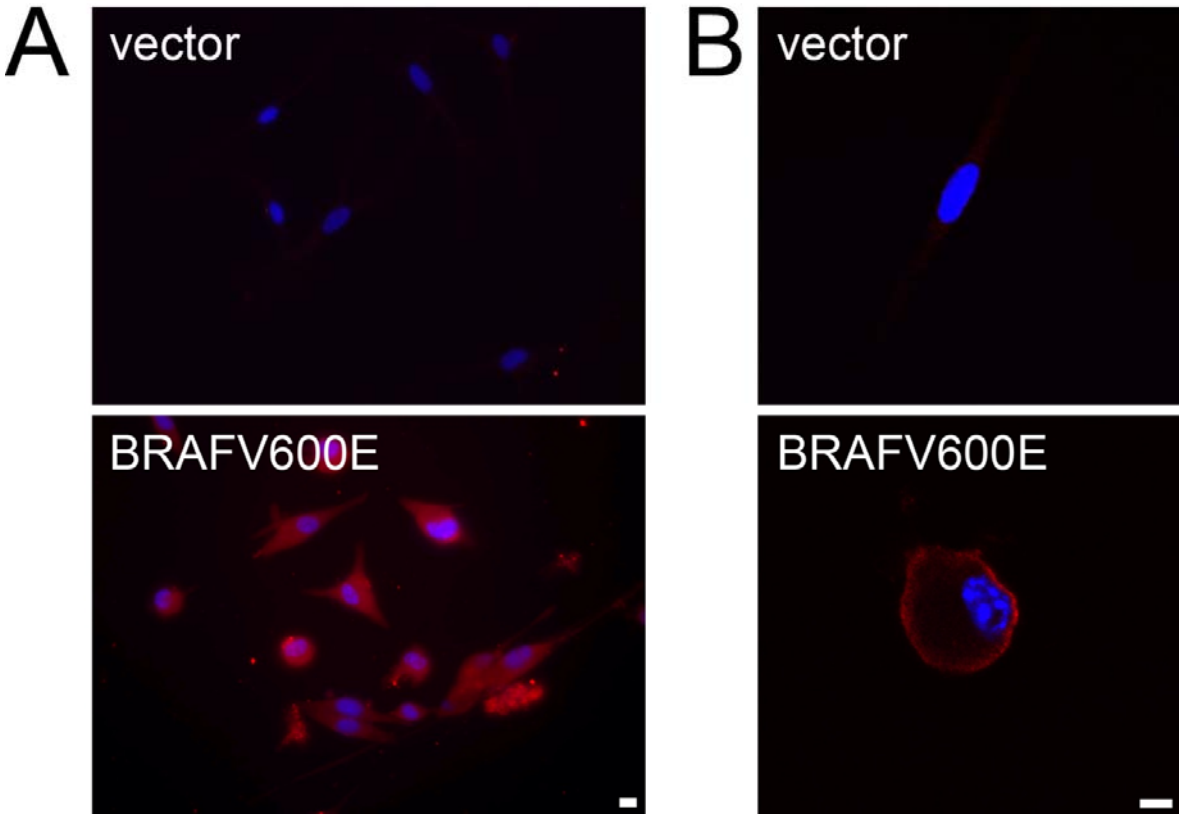

Figure S2. Immunofluorescent microscopy of HLA-DR expression on BRAFV600E expressing melanocytes.

A. Lower magnification overview IFM image of vector and BRAFV600E transduced melanocytes, showing DAPI stained nuclei in blue, and HLA-DR in red. Scale=100 µm.

B. Confocal IFM image of vector control and *BRAF*V600E expressing melanocytes, showing membrane localization of HLA-DR. Scale=100 µm.

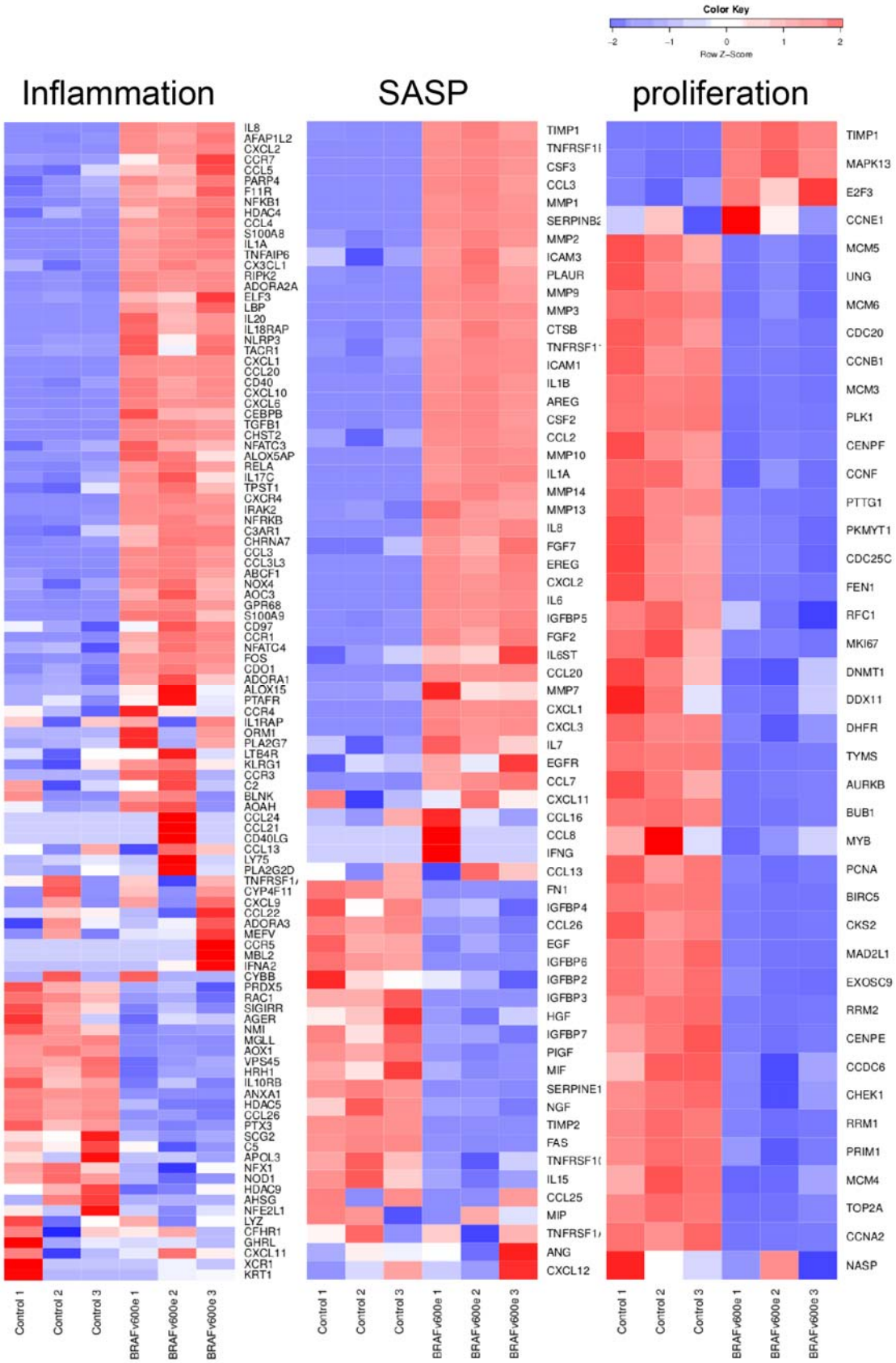
Color Key
-2
-1
0
1
2
Row Z-Score
Inflammation
SASP
proliferation
IL8
AFAP1L2
CXCL2
CCR7
CCL5
PARP4
F11R
NFKB1
HDAC4
CCL4
S100A8
IL1A
TNFAIP6
CX3CL1
RIPK2
ADORA2A
ELF3
LBP
IL20
IL18RAP
NLRP3
TACR1
CXCL1
CCL20
CD40
CXCL10
CXCL6
CEBPB
TGFB1
CHST2
NFATC3
ALOX5AP
RELA
IL17C
TPST1
CXCR4
IRAK2
NFRKB
C3AR1
CHRNA7
CCL3
CCL3L3
ABCF1
NOX4
AOC3
GPR68
S100A9
CD97
CCR1
NFATC4
FOS
CDO1
ADORA1
ALOX15
PTAFR
CCR4
IL1RAP
ORM1
PLA2G7
LTB4R
KLRG1
CCR3
C2
BLNK
AOAH
CCL24
CCL21
CD40LG
CCL13
LY75
PLA2G2D
TNFRSF1
CYP4F11
CXCL9
CCL22
ADORA3
MEFV
CCR5
MBL2
IFNA2
CYBB
PRDX5
RAC1
SIGIRR
AGER
NMI
MGLL
AOX1
VPS45
HRH1
IL10RB
ANXA1
HDAC5
CCL26
PTX3
SCG2
C5
APOL3
NFX1
NOD1
HDAC9
AHSG
NFE2L1
LYZ
CFHR1
GHRL
CXCL11
XCR1
KRT1
TIMP1
TNFRSF1
CSF3
CCL3
MMP1
SERPINB
MMP2
ICAM3
PLAUR
MMP9
MMP3
CTSB
TNFRSF1
ICAM1
IL1B
AREG
CSF2
CCL2
MMP10
IL1A
MMP14
MMP13
IL8
FGF7
EREG
CXCL2
IL6
IGFBP5
FGF2
IL6ST
CCL20
MMP7
CXCL1
CXCL3
IL7
EGFR
CCL7
CXCL11
CCL16
CCL8
IFNG
CCL13
FN1
IGFBP4
CCL26
EGF
IGFBP6
IGFBP2
IGFBP3
HGF
IGFBP7
PIGF
MIF
SERPINE1
NGF
TIMP2
FAS
TNFRSF1
IL15
CCL25
MIP
TNFRSF1
ANG
CXCL12
TIMP1
MAPK13
E2F3
CCNE1
MCM5
UNG
MCM6
CDC20
CCNB1
MCM3
PLK1
CENPF
CCNF
PTTG1
PKMYT1
CDC25C
FEN1
RFC1
MKI67
DNMT1
DDX11
DHFR
TYMS
AURKB
BUB1
MYB
PCNA
BIRC5
CKS2
MAD2L1
EXOSC9
RRM2
CENPE
CCDC6
CHEK1
RRM1
PRIM1
MCM4
TOP2A
CCNA2
NASP
Control 1
Control 2
Control 3
BRAFv600e 1
BRAFv600e 2
BRAFv600e 3

Figure S3. IMR90 fibroblasts expressing BRAFV600E display transcription profiles in compliance with senescence.

Correlation clustered heatmap of a curated list of known proliferation, inflammation and senescence associated secretory phenotype (SASP) genes. The colour intensity represents column Z-score, with red indicating high and blue low expression. The IMR90 fibroblasts were assayed 1 week after infection with BRAFV600E or control vectors.

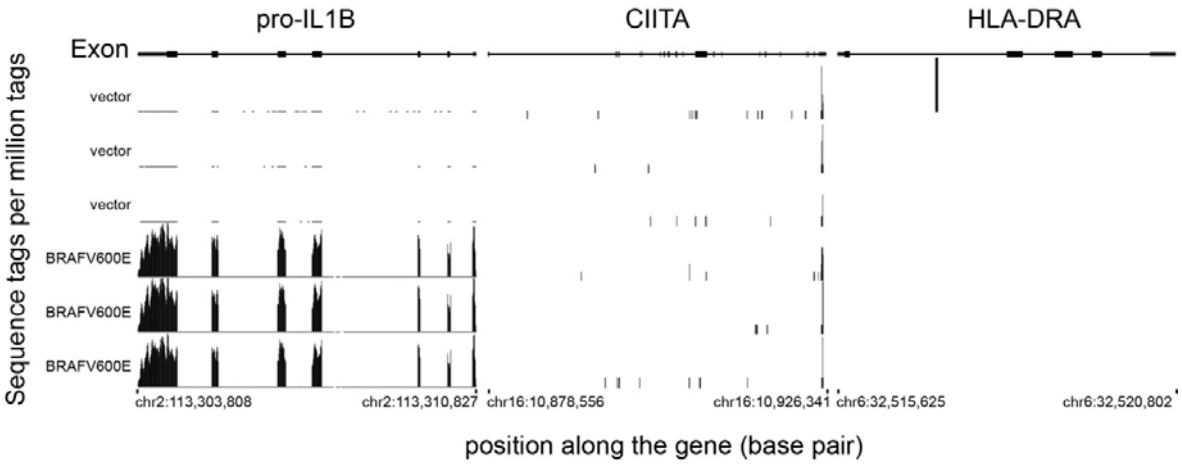

Figure S4. IMR90 fibroblasts show IL1B, but not CIITA or HLA-DRA, transcripts upon BRAFV600E expression.

Normalized RNAseq plots showing transcripts for the IL1B, CIITA and HLA-DRA genes, in IMR90 fibroblasts expressing either vector control or BRAFV600E. The IMR90 fibroblasts were assayed 1 week after infection with BRAFV600E or control vectors.

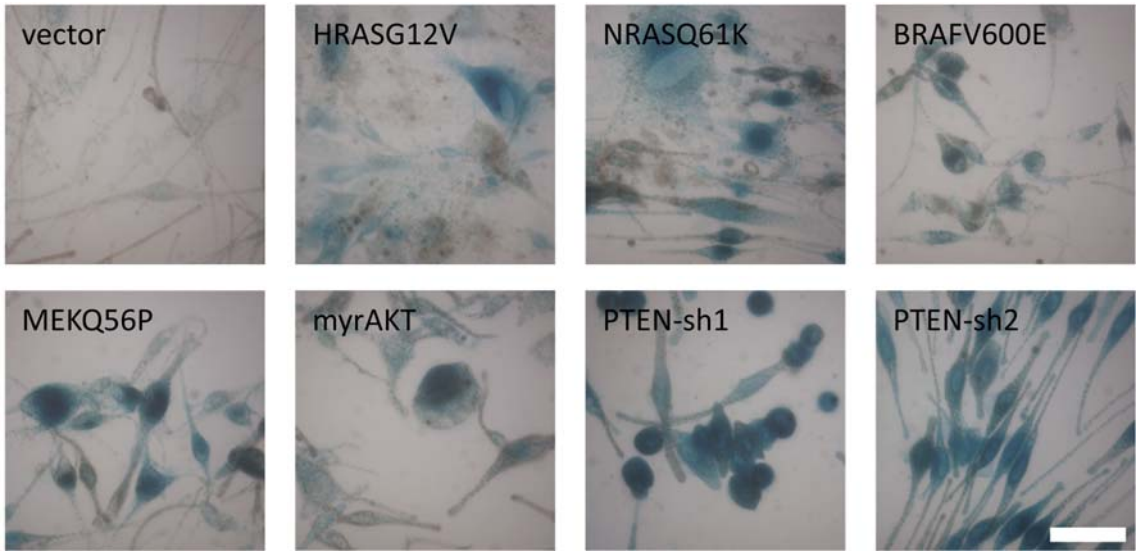

Figure S5. Oncogene induced senescence in melanocytes is accompanied by expression of senescence associated beta-galactosidase expression.

Representative staining for SA beta-galactosidase activity of melanocytes transduced with control vector, *HRAS*G12V, *NRAS*Q61K, *BRAF*V600E, *MEK*Q56P, myr*AKT* over-expression vectors and 2 different PTEN knockdown vectors for the quantified SA-Bgal counts shown in Figure 2G. Scale = 50 μm.

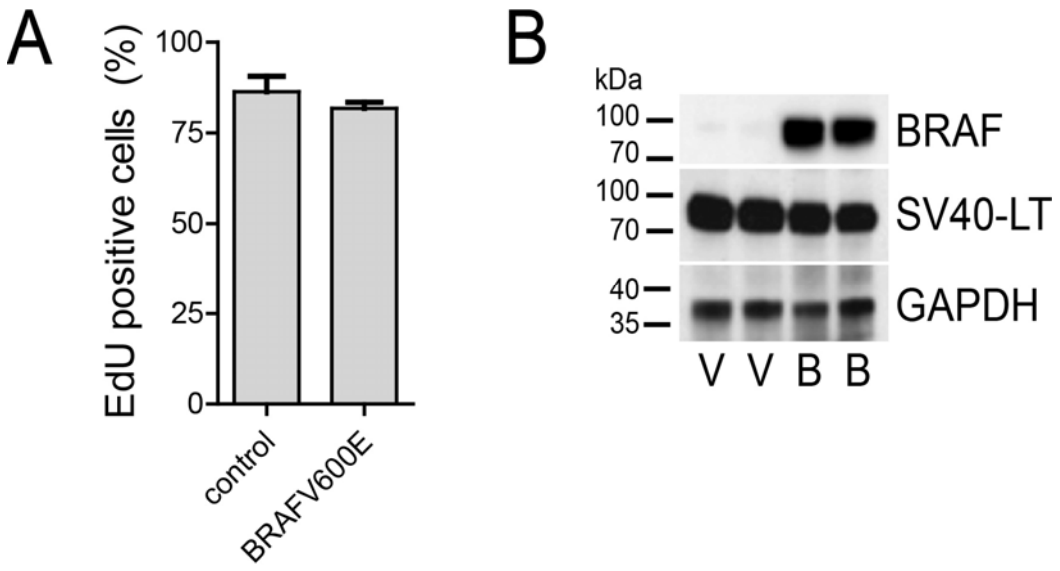

Figure S6. SV40 T-antigen can drive proliferation of melanocytes irrespective of mutant BRAFV600E presence.

A. Plot showing average percentage (n=3 +/- SD) of EdU positive melanocytes co-expressing SV40-T antigen and either vector (control) or BRAFV600E.

B. Representative Western blot showing expression of BRAF, SV40-LargeT and GAPDH as loading control.

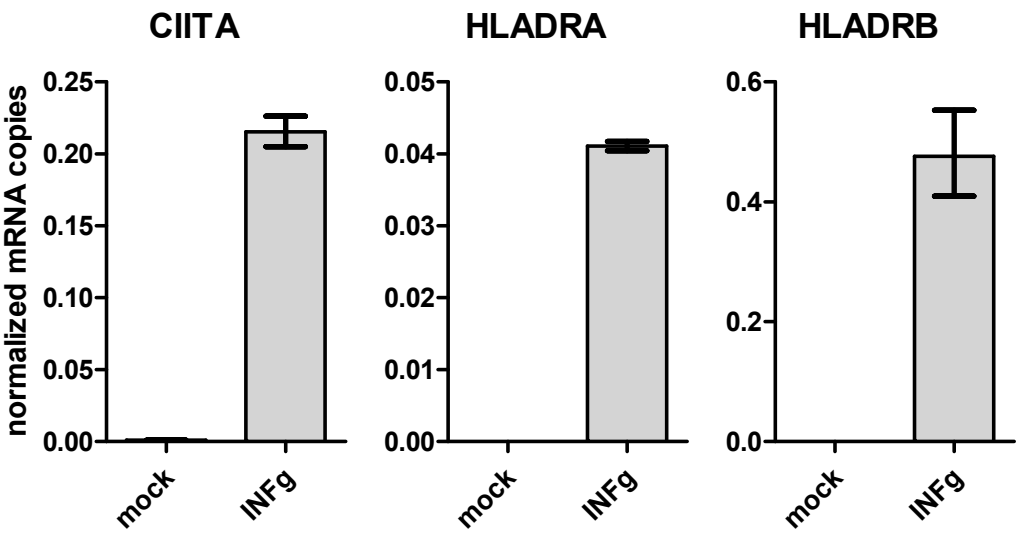

Figure S7. Interferon gamma induces CIITA and HLA-DR in melanocytes.

CIITA, HLA-DRA and HLA-DRB transcript levels detected by qRT-PCR analysis of mock or interferon gamma treated melanocytes. Graph depicts means +/- SD, n=4.

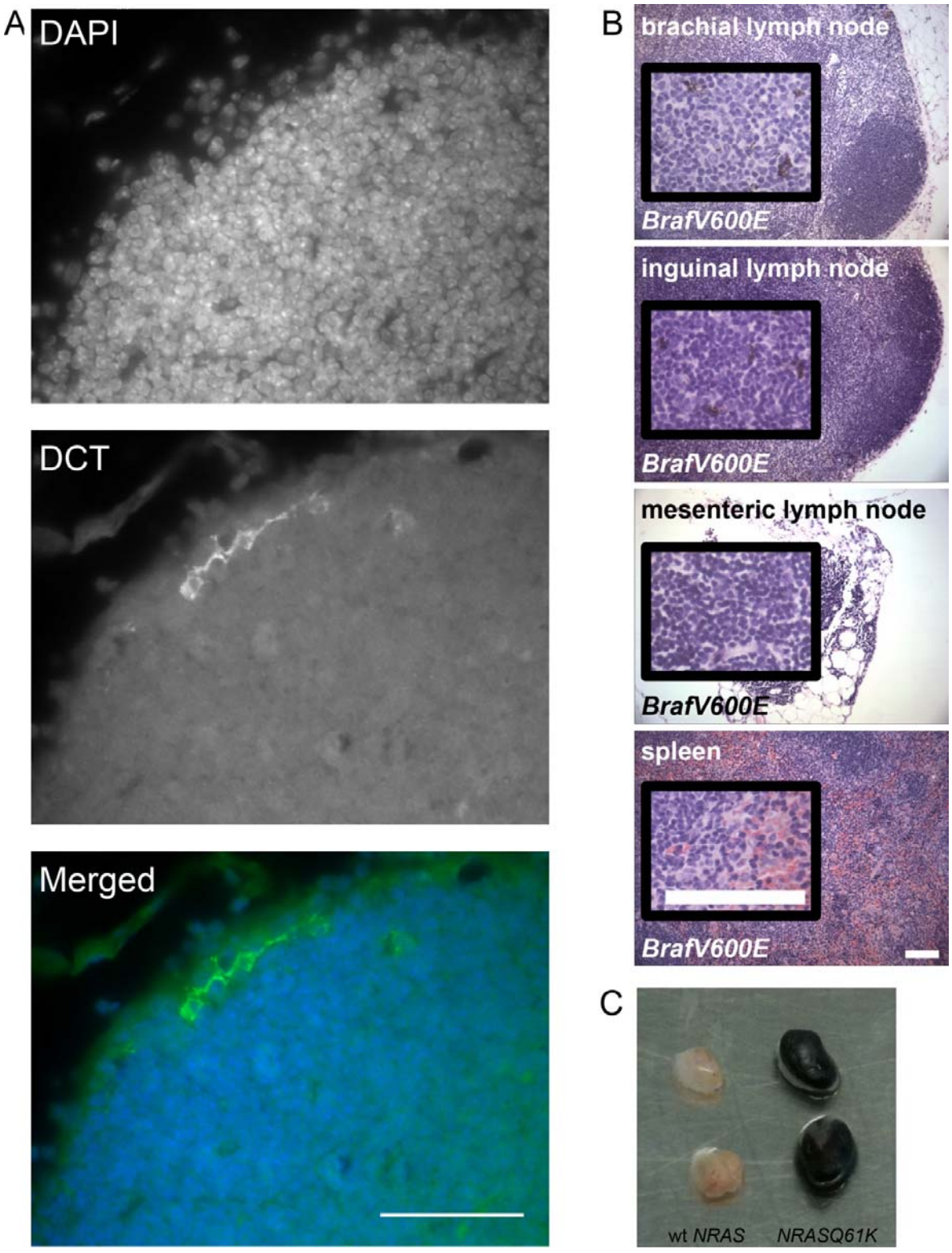
A
DAPI
DCT
Merged
B
brachial lymph node
BrafV600E
inguinal lymph node
BrafV600E
mesenteric lymph node
BrafV600E
spleen
BrafV600E
C
wt NRAS
NRASQ61K

Figure S8. *Nras*Q61K and *Braf*V600E mutant melanocytes are present in skin draining lymph nodes.

A. Dendritic DCT (green)-expressing cells (presumptive melanocytes) adjacent to the subcapsular sinus of the lymph node. DAPI, blue. Scale bar = 100 μm.

B. Haematoxylin and eosin stained sections of skin draining (inguinal and brachial) lymph nodes, non-skin draining (mesenteric) lymph nodes and spleen of WT and Tyr-CRE-ER : LSL-BrafV600E mice. Note the pigment in the inguinal and brachial nodes. Scale bar = 100 μm.

C. Representative image of prepared inguinal lymph nodes from a WT mouse and a Tyr-NrasQ61K mouse, which expresses *NRAS*Q61K under the control of the tyrosinase promoter in melanocytes.

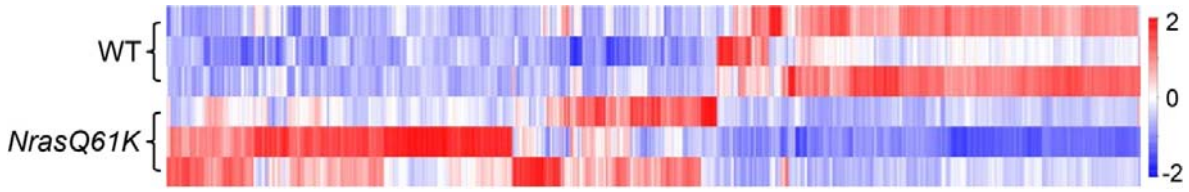

Figure S9. Differentially expressed genes between WT and *Tyr-NrasQ61K* lymph nodes.

Column clustered heatmap of differentially expressed genes (FDR <= 5%) between WT and *Tyr-NrasQ61K* lymph nodes. Genes are given by column and samples by row. The color intensity represents column Z-Score, where red indicates more highly expressed, and blue more lowly expressed genes. Heatmap shows up and down regulation of approximately 577 and 423 genes respectively.

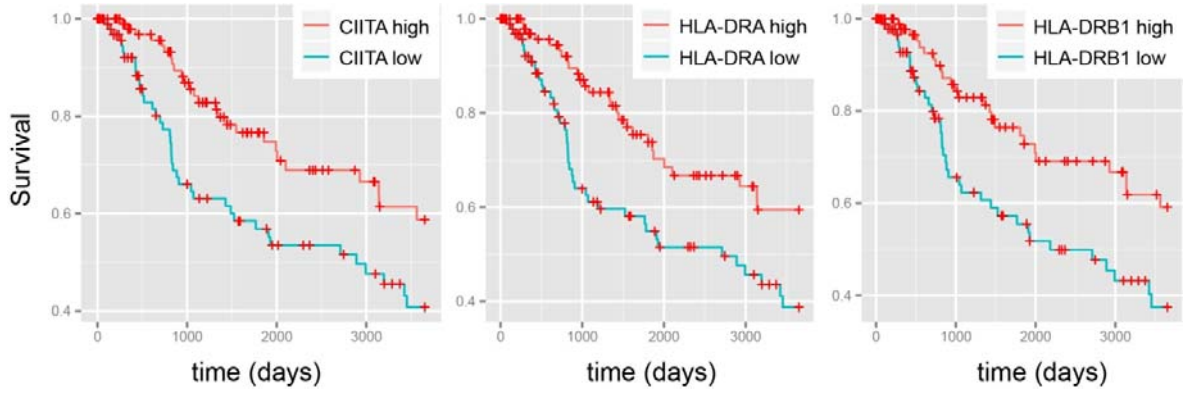

Figure S10. Skin cutaneous melanoma patient survival correlates with MHC II expression.

Kaplan Meier Curves of 10 year skin cutaneous melanoma patient survival (data from TCGA). Patients in the upper and lower quartiles of CIITA (left), HLA-DRA (middle) and HLA-DRB1 (right) expression are shown by the red and blue lines respectively ($p<0.001$, Cox Proportional Hazard Model). N=109 per quartile.

EXPANDED MATERIALS AND METHODS

Cell culture

Multiple batches of different lots of Lightly pigmented neonatal human epidermal melanocytes (Invitrogen) were cultured in medium 254 with human melanocyte growth supplement (HMGS), 100 U/ml penicillin and 100 µg/ml streptomycin (all from Invitrogen). Multiple batches of different lots of Human neonatal epidermal keratinocytes were cultured in EpiLife medium with human keratinocyte growth supplement, 100 U/ml penicillin and 100 µg/ml streptomycin (all from Invitrogen). Keratinocytes were cultured on collagen (Invitrogen) coated plates. IMR90 fibroblasts were obtained from ATCC and cultured in DMEM, supplemented with 20 % (v/v) fetal bovine serum, 100 U/ml penicillin and 100 µg/ml streptomycin (all from Invitrogen).

Lentivirus vector construction, production and infection

Lentivectors encoding CIITA, HRASG12V, NRASQ61K, BRAFV600E, MEK1Q56P, myrAKT, SV40 T-antigen or short hairpins directed against PTEN, CIITA and IL-1B, under the transcriptional control of the cytomegalovirus initial early promoter and puromycin or neomycin resistance from the simian virus 40 promoter were generated using standard methods; details available upon request. Vesicular stomatitis virus G pseudotyped lentivector stocks were produced as described previously (van Tuyn *et al.*, 2007). Melanocytes, keratinocytes and IMR90 fibroblasts were infected overnight in normal culture medium supplemented with 2 (melanocytes and keratinocytes) and 8 µg/ml polybrene, respectively overnight. Followed by 14-32 days of culture in the presence of 1 µg/ml puromycin or 250 µg/ml G418S (Invitrogen) to select for transduced cells.

In all experiments oncogene and control vector transduced cells were kept in culture under selection for 2 weeks before being assayed for senescence and gene expression as detailed below, unless stated otherwise.

Microarray, RNA-seq and analysis of TCGA data

Microarray and RNAseq analysis of melanocytes transduced with BRAF600E expression or control vectors has been described (Pawlikowski *et al.*, 2013), sequences can be obtained from the Gene Expression Omnibus (GEO) database, www.ncbi.nlm.nih.gov/geo (accession no. GSE46818).

Induction of melanocytes with conditioned medium

Cell culture supernatant was collected from BRAFV600E, vector or mock transduced melanocytes cultured in parallel at 2 weeks post transduction, and 2 days since the medium was last replaced (n=4 each). Vector transduced cultures were split several times to keep cultures at approximately the same number of cells. Culture supernatant was cleared by centrifugation at 3000 g for 10 minutes, followed by filtration through a 0.22 μm nitrocellulose membrane filter (Elkay), and frozen at -20°C until used in subsequent coculture experiments.

For the coculture experiments fresh melanocytes were cultured in parallel in a mixture of half normal culture medium as described above and half conditioned medium from either BRAFV600E, vector or mock transduced melanocytes (n=4 each). Medium was refreshed every 2 days, for a total of 2 weeks, at which time cells were harvested for RNA and RT-PCR analysis.

Induction of melanocytes with recombinant cytokines

Melanocytes were cultured in normal melanocyte growth medium (as described above), supplemented with 10 ng/ml of recombinant human Interleukin 1, beta (IL1B) (Gibco; PHC0816), recombinant human Vascular Endothelial Cell Growth Factor (VEGF) (Gibco; PHC9394), recombinant human Chemokine (C-X-C motif) ligand 1 (CXCL1) (Gibco; PHC1066), recombinant human RANTES (alternative name: CCL5) (Gibco; PHC1054), recombinant human Epithelial Neutrophil Activating Peptide-78 (ENA78, alternative name: CXCL5) (Gibco; PHC1336), or recombinant human Monocyte chemotactic protein 3 (MCP-3, alternative name: CCL7) (Gibco; PHC1574). Cells were cultured for 6 days in cytokine supplemented culture medium, which was refreshed every two days.

Genetically Modified Mouse strains

Animals were kept in conventional animal facilities and monitored frequently. All experiments were carried out in compliance with UK Home Office guidelines at the Beatson Institute for Cancer Research mouse facility (Home Office PCD 60/2607) under project license 60/4079. Mice were genotyped by PCR analysis. Mice carrying a tyrosinase promoter driven *NrasQ61K* gene (*Tyr-NrasQ61K*) have been described (Ackermann *et al.*, 2005). Mice conditionally expressing the mutant *BrafV600E* gene under control of tyrosinase driven *CRE-ER* (Delmas *et al.*, 2003) (*Tyr-CRE-ER : LSL-BrafV600E*) have also been described (Dhomen *et al.*, 2009). Albino mice carrying the *Tyr-NrasQ61K* allele were generated by cross-breeding with the albino FVB/NJ (Taketo *et al.*, 1991) strain. Control wild type mice were littermate albino mice lacking the *Tyr-NRasQ61K* transgene.

Reverse transcription-quantitative polymerase chain reaction analysis

Total RNA was isolated using the RNeasy mini spin kit with DNAse treatment (QIAGEN). Total cDNA was generated using SuperScript III (Invitrogen) from 0.1 - 5 µg RNA using

random hexamers (Invitrogen), according to manufacturer instructions. Real-time qPCR was performed on 1/50th of the cDNA, using the primers and FAM-labeled probes (IDT technologies) described in Supplemental Table S6. Reactions were performed on the Chromo4 PCR machine (Biorad), using platinum Taq, and dNTPs from Invitrogen. Transcript levels were quantified using standard curves of known quantities of plasmid DNA and normalized against the geometric mean of GAPDH and ß-actin (ACTB) gene transcripts.

Immunofluorescence microscopy

Cells were plated on glass coverslips and cultured at least 24 hours prior to fixation with 4% neutral buffered formaldehyde for 15 minutes at room temperature. Samples were washed 3 times with PBS, permeabilized with 0.1% triton in PBS for 5 minutes, followed by a further 3 washes with PBS. Cells were blocked for 30 minutes at ambient temperature with 4% bovine serum albumin and 0.02% sodium azide in PBS (blocking solution), followed by 1 to 24 hour labeling with anti HLA-DR (L243; Abcam) at 1 µg/ml in blocking solution at 4 °C. After 3 washes with PBS, cells were labeled with appropriate Alexa568 conjugated secondary antibodies (Invitrogen) in blocking solution for 1 hour at ambient temperature. Finally samples were washed 4 times with PBS and mounted in prolong gold with DAPI (Invitrogen). Images were acquired on the Nikon eclipse 80i fluorescent microscope, and the Olympus Fluoview 1000 IX81 confocal microscope.

Cytokine array

Culture supernatant from BRAFV600E and vector control transduced melanocytes was collected 2 weeks post transduction, and 2 days since the medium was last replaced. Culture supernatant was cleared by centrifugation at 3000 g for 10 minutes, followed by filtration through a 0.22 µm nitrocellulose membrane filter (Elkay). Cytokine quantities were

determined using the human cytokine array G series 3 (Raybio), according to manufacturer recommendations. Images were acquired on the Scanarray Express (Perkin Elmer).

ELISA

The human IL-1ß ESILA Kit from Thermo Scientific (EH2IL1ß) was used to measure the levels of IL1ß in the culture supernatants of Melanocytes transduced with BRAF600E or control vector following manufacturer instructions.

Immunohistochemistry

H&E staining and immunohistochemistry was performed as previously described (Pawlikowski *et al.*, 2013), using antibodies against DCT (Santa Cruz, sc-10451), FOXP3 (Abcam, ab54501) and Ki67 (Vector labs, VP-K451).

SA ß-gal and EdU assay

SA ß-gal staining was performed as previously described (Pawlikowski *et al.*, 2013). Staining for EdU incorporation was performed using the Click-iT EdU Alexa Fluor 594 Imaging kit (Invitrogen) according to manufacturer instructions, after a 72 hour pulse with EdU. Note that for all EdU experiments, a somewhat long 72 hour EdU pulse was used to truly be able to show a lack of proliferation in senescent cells, and to allow the generally slow proliferating primary cells (in the absence of BRAFV600E) used in this study to reach a significant percentage of EdU positive cells.

FACS

Fluorescence activated cell sorter (FACS) analysis was performed on a FACSCalibur system (Becton Dickinson), using standard methods. Where stated cells were stained with 5 μM

CSFE or 1 µg/ml PI, or labeled with mouse anti CD3 conjugated to allophycocyanin (Biolegend).

Mixed Leukocyte Reaction

White blood cells were isolated according to standard protocols from excess human donor buffy coats using ficoll density gradient centrifugation, and labeled for 5 minutes with 5µM CSFE at room temperature. Unincorporated CSFE was removed by three washes with PBS. WBCs were plated at a density of $1x10^5$ cells per well in 96-wells conical wells (not-cell culture treated). Melanocytes previously transduced with BRAFV600E or control vector were added to $5x10^5$ cells per well. The co-cultures were maintained for 6 days in RPMI+10% FBS, medium was refreshed daily. FACS analysis was performed to assay WBC activity.

TCGA Data

The Cancer Genome Atlas (TCGA) skin cutaneous melanoma normalized RNA-seq V2 data was downloaded from TCGA data portal (http://cancergenome.nih.gov/).

Expression correlation network of TCGA skin cutaneous melanoma data

To generate the expression correlation network (ECN) from the TCGA skin cutaneous melanoma RNA-seq V2 data (Fig 3A), firstly a matrix of expression values by gene (n = 20,531) and patient (n = 375) was generated. Next for each pairwise combination of genes, the Pearson Correlation Coefficient (PCC) of expression values across all patients was calculated. Next, to reduce the number of potentially meaningless connections two filtering steps were applied: Firstly, correlations between two genes below 0.6 were filtered out. Secondly, for each gene, correlations equal to or above 0.6 were ranked (highest first). Correlations that were not ranked amongst the top ten correlations of both genes were

removed. Finally to generate the network, the resulting data was input into an equally weighted Fruchterman-Reingold force-directed algorithm, using a k value of 0.015 and 1000 iterations. Genes were set as nodes and correlations between two genes as edges.

RNA-seq of human Melanoma and Melanocyte cell lines

Paired-end reads were aligned to the human genome (hg19) using a splicing-aware aligner (tophat2) (Kim *et al.*, 2013). Reference splice junctions were provided by a reference transcriptome (Ensembl build 73), and novel splicing junctions determined by detecting reads that spanned exons that were not in the reference annotation. Bigwig files were generated from aligned reads using library size normalization, and uploaded to the UCSC genome browser (Kent *et al.*, 2002).

RNA-seq of mouse WT and *NrasQ61K* lymph nodes

Inguinal lymph nodes were prepared from 350 day old Tyr-NrasQ61K mice and WT littermates.

Total RNA was isolated using the RNeasy mini spin kit with DNAse treatment (QIAGEN). And prepared for RNAseq according to manufacturer instructions (Illumina) and as previously described (Pawlikowski *et al.*, 2013).

Paired-end reads were aligned to the mouse genome (mm10) using a splicing-aware aligner (tophat2) (Kim *et al.*, 2013). RNAseq quality and control metrics have been listed in Table S5. Reference splice junctions were provided by a reference transcriptome (Ensembl build 74), and novel splicing junctions determined by detecting reads that spanned exons that were not in the reference annotation. Aligned reads were processed to assemble transcript isoforms, and abundance was estimated using the maximum likelihood estimate function

(cuffdiff) from which differential expression and splicing is derived (Trapnell *et al.*, 2013). Genes of significantly changing expression were defined as FDR corrected p-value <0.05.

RNA-seq Heatmaps

For each gene of biotype coding and status known in the reference transcriptome (Ensembl build 74) the FPKM value was calculated based on aligned reads, using Cufflinks (Trapnell *et al.*, 2013). Z-Scores were generated from FPKMs. Clustering was performed using the R library hclust2 and the Pearson method.

Gene Ontology analysis using David

Genes were uploaded to David (http://david.abcc.ncifcrf.gov), and a functional analysis performed using a background of Ensembl build 74 genes and the molecular functions GO terms.

Kaplan Meier Curve of 10 year skin cutaneous melanoma patient survival

The TCGA skin cutaneous melanoma normalized RNA-seq and patient clinical data was downloaded from the TCGA website (http://cancergenome.nih.gov/). Patients were filtered to include only those with both RNA-seq and clinical data, and a patient follow up date greater than 0. Patients were then grouped into quartiles by normalised CIITA, HLA-DRA and HLA-DRB1 expression level. Kaplan Meier Curves were plotted for the upper and lower quartiles of expression, using the R-library: survival (version 2.38-3). P-values were calculated using the function coxph.

Statistics

Unless otherwise specified significance was calculated using Student's t-test and graphs depict means +/- standard deviation.

SUPPLEMENTAL REFERENCES

Ackermann J, Frutschi M, Kaloulis K, McKee T, Trumpp A, Beermann F. Metastasizing melanoma formation caused by expression of activated N-RasQ61K on an INK4a-deficient background. Cancer Res 2005;65(10):4005-11.

Delmas V, Martinozzi S, Bourgeois Y, Holzenberger M, Larue L. Cre-mediated recombination in the skin melanocyte lineage. genesis 2003;36(2):73-80.

Dhomen N, Reis-Filho JS, da Rocha Dias S, Hayward R, Savage K, Delmas V, et al. Oncogenic Braf induces melanocyte senescence and melanoma in mice. Cancer Cell 2009;15(4):294-303.

Kent WJ, Sugnet CW, Furey TS, Roskin KM, Pringle TH, Zahler AM, et al. The Human Genome Browser at UCSC. Genome Research 2002;12(6):996-1006.

Kim D, Pertea G, Trapnell C, Pimentel H, Kelley R, Salzberg SL. TopHat2: accurate alignment of transcriptomes in the presence of insertions, deletions and gene fusions. Genome Biol 2013;14(4):R36.

Pawlikowski JS, McBryan T, van Tuyn J, Drotar ME, Hewitt RN, Maier AB, et al. Wnt signaling potentiates nevogenesis. Proc Natl Acad Sci U S A 2013;110(40):16009-14.

Taketo M, Schroeder AC, Mobraaten LE, Gunning KB, Hanten G, Fox RR, et al. FVB/N: an inbred mouse strain preferable for transgenic analyses. Proc Natl Acad Sci U S A 1991;88(6):2065-9.

Trapnell C, Hendrickson DG, Sauvageau M, Goff L, Rinn JL, Pachter L. Differential analysis of gene regulation at transcript resolution with RNA-seq. Nat Biotech 2013;31(1):46-53.

van Tuyn J, Pijnappels DA, de Vries AA, de Vries I, van der Velde-van Dijke I, Knaan-Shanzer S, et al. Fibroblasts from human postmyocardial infarction scars acquire properties of cardiomyocytes after transduction with a recombinant myocardin gene. FASEB J 2007;21(12):3369-79.